UCRL-53559
Distribution Category UC-21

UCRL--53559

DE86 006996

The High-Yield Lithium-Injection Fusion-Energy (HYLIFE) Reactor

Compiled by:

James A. Blink, William J. Hogan, Jack Hovingh, Wayne R. Meier, and John H. Pitts

Editors:

Kellie L. Essary
Kevin E. Lewis

Manuscript date: December 23, 1985

LAWRENCE LIVERMORE NATIONAL LABORATORY
University of California • Livermore, California • 94550

Available from: National Technical Information Service • U.S. Department of Commerce
5285 Port Royal Road • Springfield, VA 22161 • A03 per copy • (Microfiche A01)

Contents

The High-Yield Lithium-Injection Fusion-Energy (HYLIFE) Reactor

Abstract

The High-Yield Lithium-Injection Fusion Energy (HYLIFE) concept to convert inertial confinement fusion energy into electric power has undergone intensive research and refinement at LLNL since 1978. This paper reports on the final HYLIFE design, focusing on five major areas: the HYLIFE reaction chamber (which includes neutronics, liquid-metal jet-array hydrodynamics, and structural design), supporting systems, primary steam system and balance of plant, safety and environmental protection, and costs. An annotated bibliography of reports applicable to HYLIFE is also provided.

We conclude that HYLIFE is a particularly viable concept for the safe, clean production of electrical energy. The liquid-metal jet array, HYLIFE's key design feature, protects the surrounding structural components from x rays, fusion fuel-pellet debris, neutron damage and activation, and high temperatures and stresses, allowing the structure to last for the plant's entire 30-year lifetime without being replaced.

1. Introduction

When we look beyond the energy needs of the present generation, it is clear that humankind will eventually be forced to turn from hydrocarbon fuels to find longer-lasting energy sources. Of the three major possible sources of future energy—solar technology, fission breeders, and fusion—fusion is an option that merits continued intensive development.

In our relatively low-gravity terrestrial environment, fusion can be produced in two ways: by magnetic confinement and by inertial confinement. Magnetic confinement fusion (MCF) uses a magnetic field to contain a low-density plasma for a relatively long time. In contrast inertial confinement fusion (ICF) achieves the same fusion output by confining a very dense plasma with the plasma's own inertia for a necessarily short time.

ICF technology is less developed than MCF; however, it offers certain engineering advantages over MCF for the creation of a practical reactor. One major advantage is the large allowable distance between the laser or ion-beam driver and the fusion reaction chamber. This distance prevents neutron activation of the driver equipment and allows a single driver to support several reaction chambers. In addition, the driver system can be external to the reactor containment structure, allowing easier access for maintenance purposes.

Another important advantage of ICF is its comparatively relaxed vacuum requirement of ~ 10 Pa ($\sim 10^{-1}$ Torr), compared with $\sim 100\,\mu$Pa to 10 mPa ($\sim 10^{-9}$ to 10^{-6} Torr) for MCF. This relaxed vacuum requirement allows us to place a liquid-metal jet array between the fusion reactions and the structural walls to absorb the fusion neutrons, x rays, and fusion fuel-pellet debris. The liquid-metal array is the key feature of the HYLIFE reaction chamber, which is illustrated along with the associated power plant in Fig. 1. With the protection provided by the liquid metal, the first structural wall (FSW)—that wall closest to the fusion reactions—becomes appreciably less radioactive and suffers less radiation damage per unit of net energy produced than do MCF or ICF reactors with unprotected walls. The liquid metal moderates and absorbs about 90% of the neutron energy. Our research shows that with current technology and materials we can build structural walls protected by a liquid-metal jet array capable of lasting the power plant's entire 30-year lifetime.

The above advantages, plus ICF's high-power density and small containment volume, should lead to reasonably low-cost electricity.

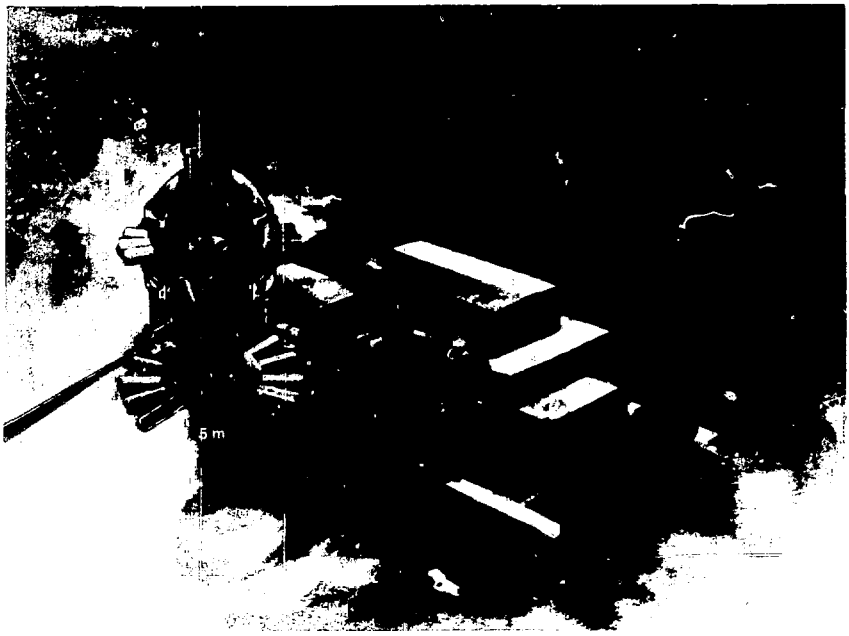

Figure 1. The HYLIFE reaction chamber and power plant. The two driver beams are shown entering the plant at the lower right side of the figure.

2. HYLIFE Reaction Chamber

2.1 Evolution of the Final Design

In 1978, we began a formal study of the HYLIFE concept at LLNL. Over the next few years, we reported on the progress of this study in the LLNL *Laser Program Annual Report* and in other scientific publications. Our goal was to develop a practical, clean reactor design that used current technology and took advantage of ICF's inherent benefits. We believe we have met our goal.

In this report, we summarize the final HYLIFE design and in Appendix A present an annotated bibliography that directs the reader to sources containing more detailed information than presented here.

The final HYLIFE design has evolved from a large number of independent studies on various aspects of the chamber and power plant, causing some inconsistencies in the magnitudes of various parameters reported in earlier publications. For this reason, parameter values given in this report should be used instead of magnitudes documented earlier. Considerable effort was put forth to make the final HYLIFE design internally consistent; detailed analyses performed at earlier design points were repeated for the final design point only when they would alter our conclusions about basic feasibility.

2.2 Summary of Final Design Parameters

The HYLIFE chamber design[1,2] uses a continuously falling liquid-metal blanket composed of 175 jets, each 0.2 m in diameter at the reactor midplane. (The HYLIFE chamber design is shown in Fig. 2, and the design characteristics are listed in Table 1.) We chose lithium as the liquid metal for our baseline design, although one other option, a eutectic containing 17 at.% lithium and 83 at.% lead, was studied. Lithium and the lithium-lead eutectic have their respective advantages. Lithium has low density, which allows low pumping power and lower stresses on the primary loop piping, and it does not become radioactive. The lithium-lead eutectic is less chemically reactive than lithium and poses less of a fire hazard; however, it does become activated.

To protect the FSW from x rays, fuel-pellet debris, and most of the neutron energy, we designed the liquid-metal jet array with an effective thickness of 0.74 m at the reactor midplane. Our calculations show that with the liquid-metal jet-array protection the total radiation damage due to helium production and displaced atoms in the FSW and nozzle plate after 30 years of plant operation would not exceed the accepted damage limits.[3-5] This long-life design offers two important advantages: It eliminates the need to periodically replace structural elements, and it reduces the total amount of activated material produced.

The jet array is arranged to allow short-wavelength-laser illumination of the fusion fuel pellet from two sides by two 6-m-tall x 2-m-wide mirror arrays mounted 60 m from the chamber center. We used an allowable mirror fluence of 20 J/cm^2 with short wavelength (1/4 to 1/3 μm), pulse-shaped laser light which has the bulk of its energy in the last 5 to 10 ns. A heavy-ion-beam driver[6] could also be accommodated, but the vapor density would need to be reduced to that needed for ballistic ion propagation. This could be accomplished by reducing the lithium temperature or by using $Li_{17}Pb_{83}$.

The jet array will completely disassemble with each fusion pulse and must be reestablished before the next pulse. Because only about 4% of the 1800-MJ fusion yield is converted to kinetic energy of liquid and gas, transient mechanical stress can be kept low. For this reason, the FSW can be designed to survive the roughly one billion fusion pulses that occur in the plant's lifetime.

The HYLIFE power plant uses heated liquid metal to operate steam generators and produce electricity. Eleven electromagnetic pumps, each with 7.8-m^3/s capacity,[7] circulate the liquid lithium through the reaction chamber. Two smaller pumps (4.9 m^3/s) force some of the lithium through four Li-Na intermediate heat exchangers (IHXs). The heated sodium (Na) from the IHXs drives 12 steam generators. The power balance of a laser-driven HYLIFE power plant is shown in Fig. 3.

To ensure safety with a minimum of operator intervention, the HYLIFE design incorporates passive features, such as filling the reactor and other surrounding rooms with inert gas to prevent fires. These features are discussed in Sec. 5.1.

HYLIFE is designed to have minimal environmental impact. The liquid-lithium coolant contains the tritium chemically, and a maximum of only a few kCi/d (about 0.01% of the tritium flow) would diffuse through the heat exchanger into the sodium (assuming zero tritium pressure in the sodium). Design features that reduce the diffusion rate, incorporate Na cold-trapping, or recover tritium from the water loop would limit tritium emissions to the environment to an acceptable level of 10 to 100 Ci/d. Use of the lithium jet array and a low-alloy steel, 2-1/4 Cr-1 Mo, produces an activated structure that can be buried as low-level waste within 50 years after the plant is shut down.

2.3 Neutronics

We used TARTNP[8] (a coupled neutron-photon Monte Carlo transport code) and LLNL's Evaluated Nuclear Data Library (ENDL)[9] to analyze the neutron-energy deposition and tritium-breeding characteristics of the HYLIFE design. The results reported in this section are for an earlier liquid-metal jet-array configuration, which had an effective lithium thickness of 1.0 m. (In the final design, the effective thickness was reduced to 0.74 m.) While the spatial distribution would be different for the final design, the overall energy deposition and tritium-breeding ratio would not change significantly.

Each DT fusion reaction produces a 14.1-MeV neutron. In ICF, this neutron is produced within a region of highly compressed DT, which can have a significant moderating effect on the neutrons. The effects of the compressed fuel in the fusion pellet on the 14.1-MeV neutrons are included in the calculation. A 14.1-MeV-neutron source is uniformly distributed throughout a spherical zone of compressed DT with a density-radius product ρR of 3.0 g/cm^2. This fuel ρR is typical of expected reactor-class fusion fuel pellets.

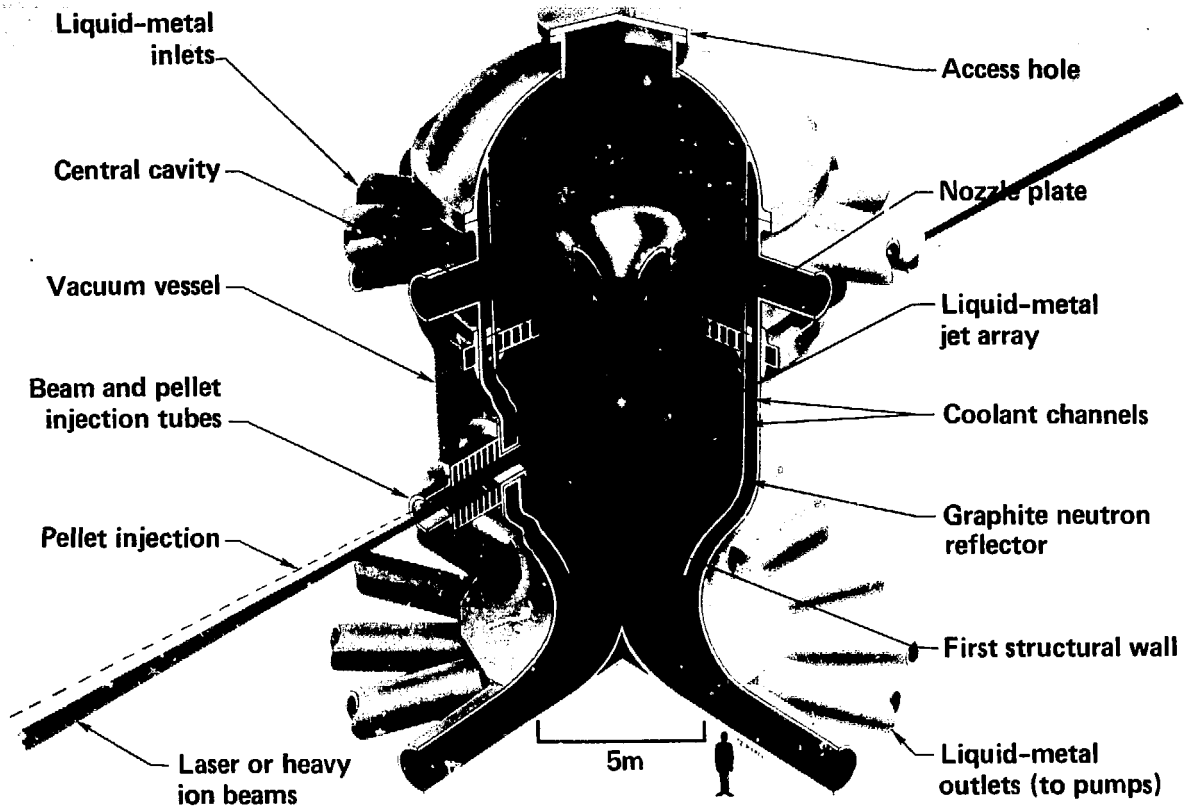

Figure 2. HYLIFE reaction chamber. The liquid lithium free falls through the nozzle plate into the vacuum chamber, forming 175 jets that protect the wall of the chamber from the damaging effects of the fusion energy pulses at its center.

Table 1. Final HYLIFE design characteristics.

System parameters	Value
Fusion power	2700 MW
Gross thermal power	3170 MW_t
Gross electric power	1240 MW_e
Net electric power	1010 MW_e
Net system efficiency	32%
Maximum tritium-breeding ratio (adjustable)	1.75
Chamber lifetime	30 y
Capacity factor	70%
Laser and pellet parameters	
Beam energy	4.5 MJ
Pellet gain	400
Yield	1800 MJ
Repetition rate	1.5 Hz
Laser efficiency	5%
Laser power consumption	135 MW_e
Miscellaneous plant power consumption	95 MW_e
Fusion chamber	
First structural wall radius	5 m
Height between the nozzle plate and the bottom of the first structural wall	8 m
Structural material	2-1/4 Cr-1 Mo
Midplane neutron flux	
without lithium	6.9 MW/m^2
with lithium	0.74 MW/m^2
Midplane neutron damage after 30 years at 70% capacity factor (limit 165 dpa)	165 dpa
Midplane neutron damage after 30 years at 70% capacity factor (limit 500 appm He)	270 appm He
Liquid-metal (lithium) array geometry	
Number of jets	175
Midplane jet diameter	0.2 m
Midplane packing fraction	0.57
Array inner radius	0.52 m
Array outer radius	1.82 m
Effective array thickness	0.74 m
Flow parameters	
Midplane jet velocity	13.3 m/s
Injection velocity	9.5 m/s
Injection head	4.6 m Li
Total head	17.6 m Li
Array lithium flow rate	72.2 m^3/s
Wall-coolant lithium flow rate	14.0 m^3/s
Intermediate heat exchanger lithium flow rate	9.8 m^3/s
Total lithium pump flow rate	96.0 m^3/s
Total lithium pumping power	22.9 MW_e
Pump efficiency	35%
Total lithium inventory	1630 m^3
Number of recirculation lithium loops	11
Lithium outlet temperature	770 K
Lithium temperature rise per pulse	18 K

The total number of neutrons leaving the pellet per source neutron is 1.06. This 6% increase in neutron population is caused primarily by the $(n,2n)$ reactions with deuterium and tritium. (For additional information on the pellet spectrum, see Ref. 10.)

The sum of the 3.5-MeV alpha-particle energy and the neutron energy deposited in the target is 5.6 MeV. This energy, which is 32% (5.6/17.6 MeV) of the fusion energy, is emitted by the pellet as x rays and as energetic debris in the form of unburned fuel, other pellet material, and the partially thermalized alpha products of the fusion reaction.

In Fig. 4, we plot the normalized neutron-fluence incident on the chamber wall for two cases. The first case is a simple geometric divergence of the target output fluence with no lithium protection. The second case includes the attenuation of an effective thickness of 1 m of lithium. The lithium zone in this comparison is a spherical shell at one-half liquid density, extending from 0.5 to 2.5 m. Although the geometry in the comparison is slightly different from the geometry in the final design, the results are indicative of the neutron-fluence incident on the midplane region of the cylindrical chamber wall. For the 2700 MW of fusion power (9.6×10^{20} DT reactions per second), the total neutron-energy fluence at 5 m is reduced from 5.7 to 0.29 MW/m^2 by 1 m of lithium shielding. The 14.1-MeV component of the neutron-fluence is reduced from 6.9 to 4.2 MW/m^2 by the compressed target and to 0.02 MW/m^2 by a 1-m-thick lithium blanket.

While the lithium blanket reduces the 14-MeV fluence by a factor of ~200 (4.2/0.02 MeV) and the total neutron-energy fluence by a factor of ~20 (5.7/0.29 MeV), the total neutron fluence is reduced by a factor of only 2. A total of 0.52 neutrons per DT reaction leaks from the lithium zone, compared to the 1.06 neutrons per DT reaction emitted by the fuel pellet. For this reason, we included a graphite neutron reflector in the HYLIFE design. The reflector moderates and reflects neutrons back into the liquid metal to be captured in ^6Li.

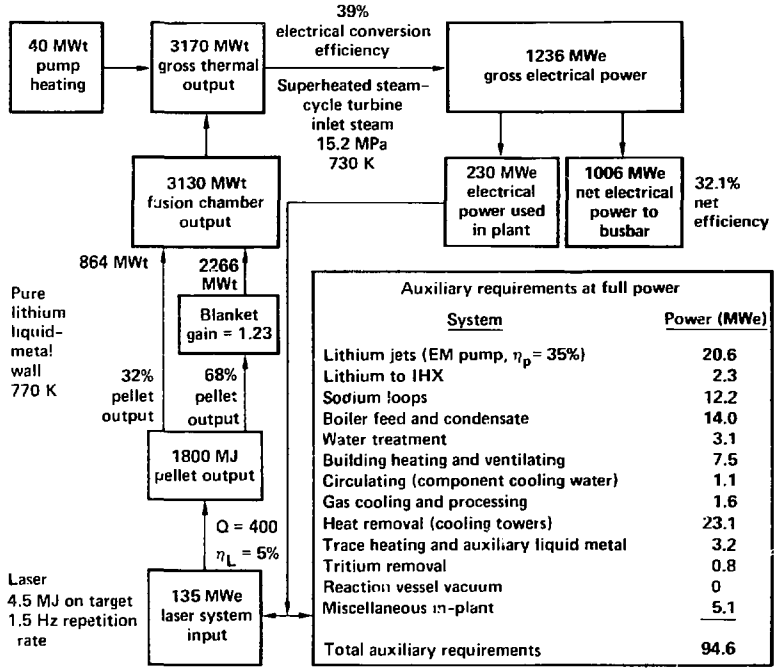

Figure 3. Power balance for a laser-driven HYLIFE power plant. The net (or system) efficiency is the net electric power divided by the fusion-chamber output power.

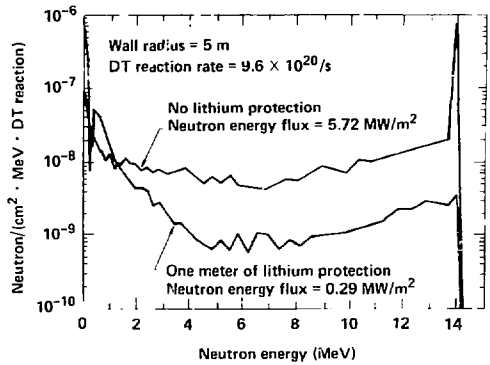

Figure 4. Neutron-fluence incident on the chamber wall for two cases: one with lithium protection and one without. The lithium reduces the overall wall fluence by a factor of ~20 and the 14-MeV fluence by a factor of ~200.

Figure 5 shows the two-dimensional (2-D) neutronics model of an earlier HYLIFE design that we find adequate to describe the final design. The numbered zones indicate different areas within the reactor. In our final design, we removed the orifice plate (zone 13) and the splash baffle (zone 17), however, the effect on the overall neutronics is insignificant.

The vertical dashed line at the left of Fig. 5 is the axis of rotation. Zone 2 represents the envelope of the jet array, which contains natural lithium at an average packing fraction of 50%. Zone 4 represents a 5-cm-thick cylindrical sh[illegible] of lithium that flows down the inner surface of the FSW to provide cooling. Zones 6 and 8 are 5-cm-thick liquid-metal coolant channels for the outer surface of the FSW, the graphite neutron reflector, and the inner surface of the vessel wall. The coolant channel between the graphite reflector (zone 7) and the vacuum-vessel wall (zone 9) also functions as a shield to absorb thermal neutrons that leak from the graphite reflector.

Zone 10, the nozzle plate, consists of a homogeneous mixture of 60% lithium and 40% ferritic steel. Zone 13 the orifice plate (eliminated in the final design), is a homogeneous mixture of 90% lithium and 10% ferritic steel. In this model, the graphite access plug (zone 12) is positioned above the hole in the center of the nozzle plate and is directly exposed to the fusion radiation. The final HYLIFE design directs one liquid jet over the nozzle-plate hole to protect the top of the chamber; this allows us to eliminate the graphite access plug. (See Fig. 2.) Zone 18, the outlet pool, and

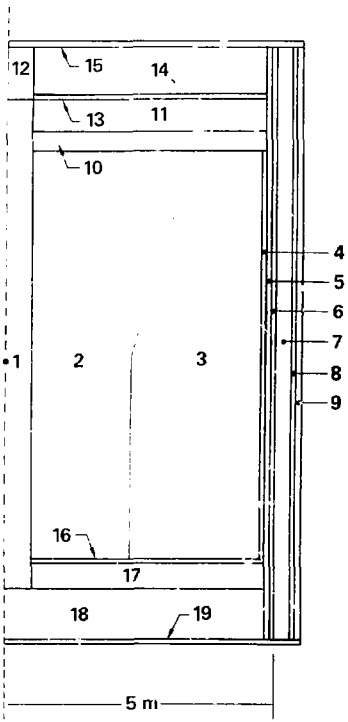

Zone number	Region description, material
1	Inner region, lithium vapor
2	Jet array, lithium at half density
3	Outer region, lithium vapor
4	Wall coolant, lithium
5	First structural wall, ferritic steel
6	Coolant channel , lithium
7	Graphite neutron reflector
8	Coolant channel and shield, lithium
9	Vacuum vessel wall, ferritic steel
10	Nozzle plate, ferritic steel
11	Injection pool, lithium
12	Graphite access plug
13	Orifice plate, ferritic steel
14	Inlet pool, lithium
15	Vessel top, ferritic steel
16	Lithium layer
17	Splash baffle, ferritic steel
18	Outlet pool, lithium
19	Vessel bottom, ferritic steel

Figure 5. Two-dimensional neutronics model. The dashed line is the axis of rotation. The compressed fuel pellet, represented by the dot near the label for zone 1, is included in the neutronics calculations.

zone 14, the inlet pool, are each 1 m thick. The inlet pool in the final design is 4.6 m thick, but again this difference has little effect on the neutronics calculations since very few neutrons reach this zone.

We did not find it necessary to include the beam-port penetrations in this early neutronics model (although they were included in some later models). Allowing approximately 0.5% of the solid angle for beam ports would reduce the tritium-breeding ratio and neutron-energy deposition by less than only 1%, which is insignificant.[11,12]

2.3.1 Energy Deposition

The distribution of neutron, gamma, and total energies deposited within each zone of the HYLIFE reaction chamber is given in Table 2. A total of 14.760 MeV per DT reaction is deposited in the chamber zones as a result of neutron interactions, which is 3.0 MeV more than the neutron-energy output of the fuel pellet. This energy multiplication is due primarily to exoergic reactions with ^{6}Li:

$$^6\text{Li} + \text{n} \rightarrow {}^4\text{He} + \text{T} + 4.8\ \text{MeV} \qquad (1)$$

Adding the 5.6 MeV that is deposited in the fuel pellet from neutrons and alpha particles gives a total energy deposition of 20.4 MeV per DT reaction. The system energy multiplication factor is thus 1.16 (20.4/17.6 MeV). Magnetic fusion reactor designers use the blanket gain rather than the multiplication factor as a figure of merit; for HYLIFE (Fig. 3), this number is 1.23 (14.760/12.0 MeV).

The fusion energy yield for the HYLIFE design (1800 MJ) times the system energy multiplication factor (1.16) gives the amount of energy deposited in the system per pulse (2090 MJ). At a pulse repetition rate of 1.5 Hz, the chamber power is 3130 MW_t. An additional 40 MW_t from pump heating in the lithium circulation and heat-transfer loops raises the total thermal power to 3170 MW_t (Fig. 3).

As indicated in Table 2, the majority of the neutron and photon energy is deposited directly in the liquid-metal jet array (in less than 1 μm).[13] In addition, essentially all of the x-ray and debris energy is absorbed in the jet array, which results in approximately 18.5 MeV of the total 20.4 MeV being absorbed in this region. When we add the energy deposited in the other liquid-metal zones, the result is approximately 19.7 MeV, or more than 96% of the total system heat load deposited directly in the liquid-metal coolant.

Table 2. Energy deposited in the chamber zones per source neutron. The gamma energies are from (n,γ) reactions; they do not include x-ray energy from the fusion pellet.

Zone number	Region description	Neutron (MeV)	Gamma (MeV)	Total (MeV)
1	Inner region	[a]	[a]	[a]
2	Jet array	12.557	0.299	12.856
3	Outer region	[a]	[a]	[a]
4	Wall coolant	0.235	0.008	0.243
5	First structural wall	0.012	0.120	0.132
6	Coolant channel	0.468	0.004	0.472
7	Graphite neutron reflector	0.073	0.051	0.124
8	Coolant channel/shield	0.205	0.001	0.206
9	Vacuum vessel wall	0.001	0.019	0.020
10	Nozzle plate	0.111	0.058	0.169
11	Injection pool	0.047	0.006	0.053
12	Graphite access plug	0.023	0.007	0.030
13	Orifice plate	0.006	0.001	0.007
14	Inlet pool	0.021	0.002	0.023
15	Vessel top	[a]	0.001	0.001
16	Lithium layer	0.059	0.002	0.061
17	Splash baffle	0.195	0.045	0.240
18	Outlet pool	0.119	0.003	0.122
19	Vessel bottom	[a]	0.001	0.001
	Total	14.132	0.628	14.760

[a]Negligible.

2.3.2 Tritium Breeding

Not only is the liquid-metal blanket the primary coolant and heat transfer medium for HYLIFE, but it serves as the source of tritium needed for the fusion fuel. Tritium is bred from the two isotopes of natural lithium, 7.4% ^{6}Li and 92.6% ^{7}Li, by the following neutron reactions:

$$^6\text{Li} + \text{n} \rightarrow {}^4\text{He} + \text{T} + 4.8\ \text{MeV} \qquad (2)$$

$$^7\text{Li} + \text{n} \rightarrow {}^4\text{He} + \text{T} + \text{n}' - 2.5\ \text{MeV} \qquad (3)$$

Figure 6 shows the cross sections of these two reactions. The ^{7}Li reaction is important because it produces a tritium atom and a lower-energy neutron that subsequently can breed more tritium with ^{6}Li; this reaction is only possible for neutrons

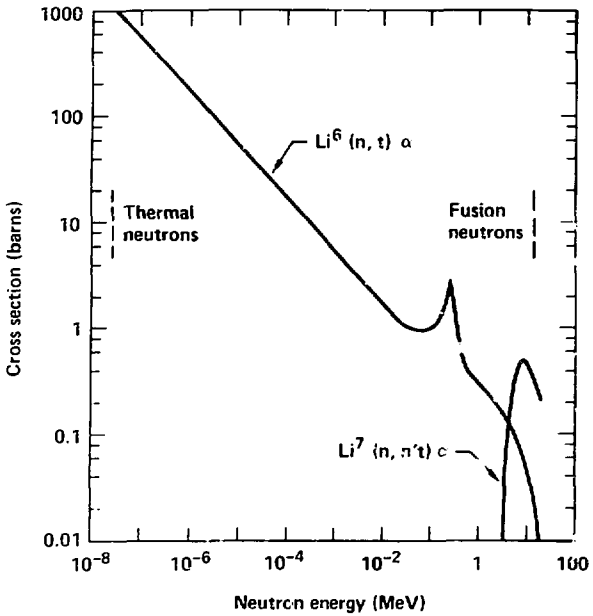

Figure 6. Cross sections for tritium-breeding reactions in lithium. The high-energy ^{7}Li reaction does not absorb the neutron; hence, a tritium-breeding ratio greater than 1 is possible.

with energies above 2.5 MeV. The HYLIFE blanket design maximizes the number of ^{7}Li(n,n'T) reactions by exposing a high volume of lithium to high-energy neutron fluence from the fusion fuel pellet. The thick liquid-metal blanket also thermalizes and absorbs neutrons in tritium-producing reactions with ^{6}Li. The graphite reflector provides further thermalization and reflects neutrons back into the interior lithium zones. Most thermal neutrons leaking outward from the graphite reflector are absorbed in the liquid-metal zone between the reflector and vacuum-vessel wall. Thus, the HYLIFE configuration tends to maximize the tritium-breeding ratio.

The tritium-breeding results for the 1-D calculation using natural lithium are given in Table 3, which lists the number of tritium-producing reactions per source neutron for each zone that contains lithium. The total of 1.75, given at the bottom right corner of the table, indicates that HYLIFE produces 75% more tritium than is needed to maintain its fuel supply. The excess tritium can be used as fuel for other types of DT fusion reactors, including D-^{3}He fusion reactors (tritium decays to ^{3}He), fusion-fission hybrids, synthetic fuel producers, and actinide burners. If a market for the excess tritium fails to develop, the HYLIFE concept can be modified to reduce the tritium-breeding ratio while maintaining its important features.[14]

Little can be done to decrease the ^{7}Li contribution to the tritium-breeding ratio, but several modifications can reduce the number of ^{6}Li(n,T)α reactions to produce the desired breeding ratio (between 1.0 and 1.75, depending on the demand for excess tritium):

- A neutron poison can be introduced into the liquid-metal stream to compete for thermal neutrons.
- The thickness of the liquid-metal blanket can be reduced.
- Neutrons can be prevented from reflecting back into liquid-metal zones.

Table 3. Tritium-breeding distribution. The ^{7}Li reactions account for 39% of the tritium breeding, while 34% of the breeding occurs in the jet array.

Zone number	Region description	T_6	T_7	$T_6 + T_7$
2	Jet array	0.808	0.666	1.474
4	Wall coolant	4.1×10^{-2}	2.3×10^{-3}	0.043
6	Coolant channel	9.3×10^{-2}	1.2×10^{-3}	0.094
8	Coolant channel/shield	4.2×10^{-2}	1.6×10^{-4}	0.043
10	Nozzle plate	1.9×10^{-2}	6.4×10^{-4}	0.020
11	Injection pool	7.4×10^{-3}	7.1×10^{-4}	0.008
13	Orifice plate	8.8×10^{-4}	6.5×10^{-5}	0.001
14	Inlet pool	3.1×10^{-3}	3.2×10^{-4}	0.003
16	Lithium layer	1.0×10^{-2}	6.0×10^{-4}	0.011
17	Splash baffle	3.4×10^{-2}	1.5×10^{-3}	0.036
18	Outlet pool	1.4×10^{-2}	4.1×10^{-3}	0.018
	Total	1.072	0.679	1.75

$^aT_6$ = ^{6}Li(n,T)α reactions per source neutron.
T_7 = ^{7}Li(n,n'T)α reactions per source neutron.

- The isotopic concentration of ^{6}Li in lithium can be reduced.
- A combination of the above modifications can be used.

The most attractive potential modification to reduce the number of ^{6}Li(n,T)α reactions is to reduce the isotopic concentration of ^{6}Li to approximately 0.1% and replace the graphite reflector with boron carbide. Although this modification increases the neutron flux to the chamber wall, which causes increased neutron damage, heat load, and thermal stress in the chamber wall, it does have a number of important advantages. It reduces the number of ^{6}Li reactions in the liquid-metal blanket, captures leakage neutrons in ^{10}B instead of in ^{6}Li, and maintains a thick blanket while reducing the tritium-breeding ratio to approximately 1.0. Maximizing the ratio of ^{7}Li reactions to ^{6}Li reactions for a tritium-breeding ratio of 1.0 also provides for the most efficient use of the Li resources.

2.3.3 Radiation Damage

Radiation damage in the FSW results primarily from helium production and atomic displacements. Significantly moderating the neutron spectrum with the liquid-metal jet array reduces the radiation damage rates because the helium-production and atomic-displacement-damage cross sections for the major constituents of common ferritic steels decrease rapidly with decreasing neutron energy (Fig. 4). To reduce radiation damage in the FSW, we selected a liquid-metal jet-array thickness that would moderate the neutrons and absorb a high percentage of them.

The lifetime of a 2-1/4 Cr-1 Mo ferritic steel FSW as a function of the thickness of liquid-metal protection is shown in Fig. 7. The allowable damage limits used are 500 atomic parts per million (appm) of helium production and 165 displacements per atom (dpa). These radiation damage limits are discussed in Refs. 3 and 15. A lifetime of 21 full-power years (30 years at a 70% capacity factor) can be reached with a liquid-lithium jet-array thickness of 74 cm.

The damage rates used to generate the curves in Fig. 7 were based on early, one-dimensional neutronics calculations with a solid-annular Li zone that has an inner radius located 2 m from the center of the reaction chamber.[3,15] The liquid-metal jet array in the final HYLIFE design is much closer to the center of the reaction chamber. Recent neutronics calculations showed that the position of the Li blanket within the reaction chamber has a significant effect on the radiation damage rates in the FSW.[16] That is, the damage rates increase as the Li blanket is moved closer to the center of the chamber.

Because the liquid-metal jet array in the final HYLIFE design is much closer to the center of the reaction chamber, the lifetime of the FSW would be somewhat less than indicated in Fig. 7. If the damage limits are correct, HYLIFE would require an additional 10- to 15-cm Li thickness (84 to 89 cm instead of the previously mentioned 74 cm) to increase the FSW lifetime to 21 full-power

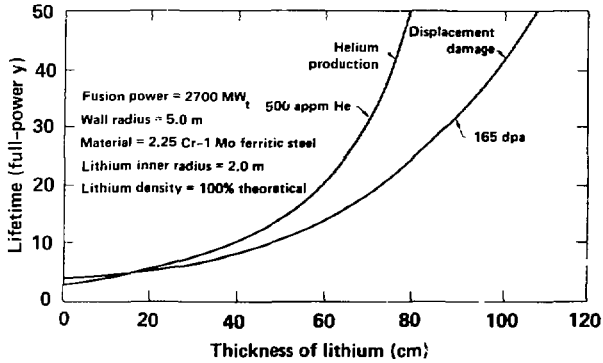

Figure 7. Lifetime of the first structural wall as a function of the thickness of the lithium protection. For Li thickness >15 cm, displacement damage (rather than He production) is the life-limiting phenomenon.

years. However, these damage limits are quite uncertain. The 165-dpa limit had been suggested for 316 austenitic stainless steel, but the 2-1/4 Cr-1 Mo ferritic steel is expected to be more resistant to the effects of displacement damage because it swells less than stainless steel. For this reason, the dpa limit might be significantly higher than 165. A higher damage limit would allow a thinner Li jet array, offsetting the geometric effect.

With such uncertainties about the radiation damage limits, we cannot precisely specify the liquid-metal jet array thickness. However, the technique used is more important than the precise thickness. The intention of the designers is to minimize the jet-array thickness subject to the constraint that, from radiation damage considerations, the FSW will last for the life of the power plant.

Further discussion of the compatibility of materials for HYLIFE is presented later in this report.

2.4 Liquid-Metal Jet-Array Hydrodynamics

The most novel part of the HYLIFE concept is the liquid-metal jet array. In this section, we will describe the jet array's response to the fusion pulses and the consequent wall stresses, the feasibility of establishing the jet array from a nozzle plate, the stable length of the individual jets, the beam aperture design, and pulse-rate limitations.

2.4.1 Hydrodynamic Response to Fusion-Energy Deposition

Early liquid-metal-fall designs evolved into the final HYLIFE design: a closely packed, annular jet array. The annular jet array is preferable to a continuous annular fall because large pressures are not able to build up inside the array. The high-pressure plasma is vented into a larger chamber volume without accelerating the liquid to unreasonable velocities.[17]

Figure 8 shows the hydrodynamic response of the liquid-metal jets as a function of time, and Table 4 shows a chronology of events for one HYLIFE pulse. Initially the jet array extends from a radius of 0.52 to 1.82 m and has a midplane packing fraction of 57%. Energy from each fusion pulse is deposited isochorically (at constant volume) in the liquid-metal jet array. Most of the x-ray and pellet-debris energy is deposited in the first few microns of liquid metal closest to the fuel pellet; this liquid metal vaporizes and converges toward the chamber center. The vaporization drives a shock into the inner jets, resulting in high-velocity, rear-surface spall; however, the outer jets absorb the spall, preventing high-velocity, erosive impact on the FSW.

Neutron energy is deposited more uniformly throughout the liquid-metal jet array than the x-ray and pellet debris energy. However, the neutron-energy deposition is still 10 to 100 times higher at the inner radius of the liquid-metal jet array than at the outer radius.

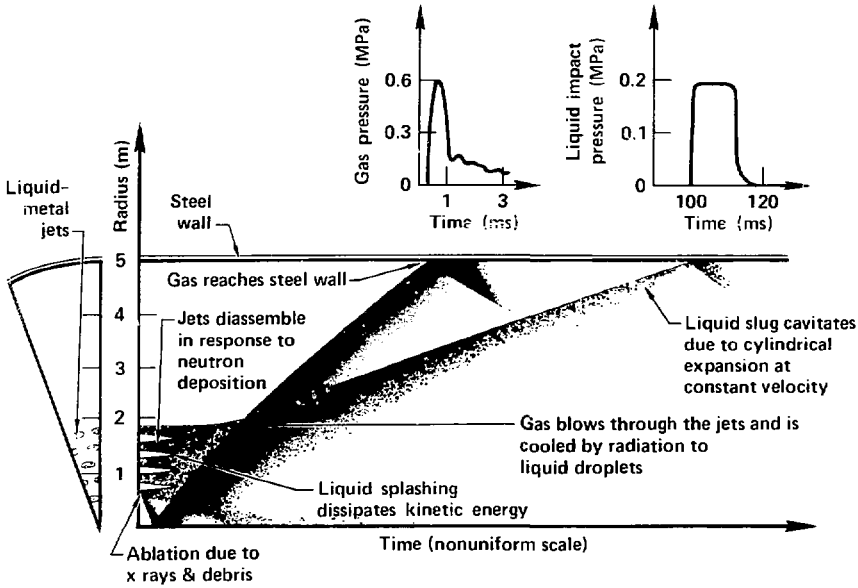

Figure 8 Hydrodynamic response to fusion-energy deposition in HYLIFE (1800-MJ yield). The peak gas pressure of 0.6 MPa produces a 38-MPa stress in the 40-mm-thick FSW, and later the liquid impact pressure of 0.2 MPa produces a 46-MPa stress in the FSW.

The thin layer of liquid metal that vaporizes forms a high-pressure plasma that moves to the center of the reaction chamber, where it stagnates and then expands back toward the jet array.[18] The jet array allows the high-pressure plasma to blow through the gaps between the jets and to transfer most of its thermal energy to the cooler liquid-metal jet array,[19] which by this time has fragmented into droplets due to the neutron heating.[20] High pressures initially in the gas are relieved by this expansion and cooling, causing the outward acceleration of the liquid-metal jet array by the gas to be small.[17]

The kinetic energy produced when the jets disassemble into liquid droplets[20] converts back to thermal energy as the droplets splash against one another. The net neutron-induced momentum of each jet row is zero, with about half of the liquid traveling inward and half outward.[21] But the inner row absorbs much more neutron energy and, therefore, its inward and outward momenta are much higher than that of the other rows. Thus, the outward portion of the inner row overwhelms the inward portion of the second row, the combined mass catches the outward portion of the second row, and so forth. Eventually, the outward momentum from the inner-jet row is distributed among the full array as it catches the slower outer jets. This leads to a relatively slow-moving, recompacted annulus, coasting at constant velocity toward the FSW. The annulus cavitates as it moves to the wall because it is in diverging geometry, with no significant forces available to preserve its density by slowing the leading edge or accelerating the trailing edge.

Structural loading of the FSW results from the vented gas pressure and, later, from impact by the cavitated liquid. Gas pressure reaches a peak of only 0.6 MPa, and pressure from the cavitated liquid impact reaches only 0.2 MPa. For the gas impact, the wall stresses are associated with the impulse (the product of pressure and time) because the FSW vibrational period (~5 ms) is much larger than the time span over which the

Table 4. **Chronology of events in one HYLIFE pulse cycle.**

Time	Event
15 ms	Deuterium-tritium fuel pellet enters the reaction chamber.
30 ns	Pellet is 5 mm from the chamber center and the laser beam enters the chamber.
15 ns	Laser beam contacts the fuel pellet.
0	Implosion is complete; fusion begins.
10 ps	Fusion burn is complete.
2 ns	X rays begin to ablate lithium.
1 μs	Neutron absorption is complete
20 μs	X ray and thermally ablated lithium reaches maximum compression at center of chamber.
40 μs	Jet fragmentation due to neutron absorption begins.
60 μs	Re-expanding lithium gas reaches the fragmenting jets.
300 μs	Expanding lithium gas clears the fragmenting jets.
400 μs	Lithium gas impacts the wall.
35 ms	Lithium liquid impacts the wall.
250 ms	Chamber pressure reduces to 10 Pa (10^{-1} Torr).
630 ms	New lithium jets are established.
652 ms	Next fusion fuel pellet enters the chamber.
666 ms	Next laser beam enters the chamber.
666 ms	Next fusion begins.

pressure is applied (<1 ms for most of the impulse). For the liquid impact, the vibrational period is shorter than the pressure pulse (the duration of which, due to cavitation, is set by the fluid velocity rather than wave velocity), and the stress is not as high as in a situation where the same impulse is applied over a short time. This is because, for about one-half of the time, the wall vibrational motion is in the opposite direction from the liquid flow, causing FSW deceleration rather than acceleration.

FSW stresses are produced when the 0.6-MPa gas pressure produces a 38-MPa stress in a 4-cm-thick wall. The liquid-impact pressure produces a 46-MPa stress in the wall several milliseconds later. A wall thickness of 4 cm was chosen to reduce the (essentially steady) thermal stress to 77 MPa, the stress having been caused by the volumetric neutron- and gamma-ray wall heating coupled with surface cooling. The peak-combined thermal and impact stress (123 MPa) is well below the 168-MPa yield strength of 2-1/4 Cr-1 Mo ferritic steel. Both the gas and liquid impact stresses are less than 40% of the 126-MPa fatigue strength.

These stress values result from our detailed hydrodynamic calculations, which emphasize two major areas: (1) the stress-reducing effects of segmenting the liquid-metal wall [17,22] and (2) the effects on wall stress[19,23] and condensation time[19] due to heat and mass transfer between the ablated gas and the bulk liquid. We also used an analytical model that was normalized to our hydrodynamic calculations to obtain the results for the final HYLIFE design.[24,25] This model allowed us to analyze a wide number of options and to minimize the liquid-metal jet-array flow rate. We then selected a final design that satisfied hydrodynamic and other constraints without performing further detailed hydrodynamic calculations.

Our first detailed hydrodynamic analysis was for an unsegmented annular fall. The wall stress was extremely high because of a high level of neutron-induced liquid momentum and because of the lack of venting.[26-29] Segmenting the fall into multiple concentric annuli reduced the net-radial, neutron-induced momentum to manageable levels.[22] Segmenting the fall into jets also vented the gas, and the drag caused by the vented gas accounted for about 20% of the liquid's radial momentum.[17,18] (The venting was modeled as gas flow through a variable cross-section nozzle.[17])

A one-dimensional analysis[19] of the interactions between the venting gas and the fragmenting liquid showed that radiation-heat transfer (primarily with the first row of jets) transfers over 70% of the gas thermal energy to the liquid. An additional 7 to 10% of the gas energy is used to vaporize liquid during venting, increasing the gas mass by 40 to 60%. A subsequent 2-D (radial-axial) analysis[23] of the heat and mass transfer showed that 2-D effects reduced the gas loads on the structure by a factor of 5 to 10, depending on the heat and mass transfer assumptions used. We also considered using quasi-rectangular jets arranged to produce tangential liquid and gas motion (instead of purely radial motion), but the potential improvement was not quantified.[30]

2.4.2 Jet Stability

The depth of the liquid-metal pool above the nozzle plate was set so that the initial jet velocity was just large enough to reestablish the jets within the desired interpulse time. The associated midplane packing fraction was 57%. A larger initial velocity would result in a larger midplane packing fraction because the jet diameter contracts less due to the acceleration of gravity. But the larger initial jet velocity also results in a larger liquid-metal flow rate.

Jet stability[31-46] was studied both analytically and experimentally. Water-jet experiments and the jet-stability analyses verified that round jets at least 20 cm in diameter would be stable for the 8-m fall lengths in the HYLIFE reactor, even when high vibration levels are imposed on the nozzle plate. Experiments involving transverse-vibration-induced collisions between two adjacent round jets showed the jets would also remain stable for the necessary length, even with large jet-velocity differences.[44-46] Consequently, the expected differences in the depth of the liquid-metal pool above the nozzle plate (due to vibrations in the nozzle plate) should not cause jet break-up problems in HYLIFE.

The stability analyses also showed that rectangular cross-section jets would not oscillate (alternate major and minor axes) in the 8-m fall distance below the nozzle plate. These rectangular jets offer a higher packing fraction than round jets.[44-46]

2.4.3 Beam Apertures

We used a set of 20 crisscrossing, liquid-metal jets to establish a flow pattern that allows the two-laser or ion-beam arrays to reach the fuel pellet unobstructed while leaving no area of the chamber wall unprotected. Ten jets (two of these are shown in Fig. 9) are crossed over each beam, five jets to a side, to form a gothic archway of liquid metal. This archway protects the nozzle plate and part of the chamber wall above the beam while forming a narrow passageway for the beam.

A triangular region of the FSW above the beam and a rectangular strip below the beam are not shielded from neutrons by the crossing jets. These areas of the FSW are therefore removed. Lithium flows through a ducting system located between the FSW and the graphite reflector to fill the upper triangle. Then, the ducting directs the flow into the chamber just below the beams, filling the lower rectangle. Figure 9 shows the beam

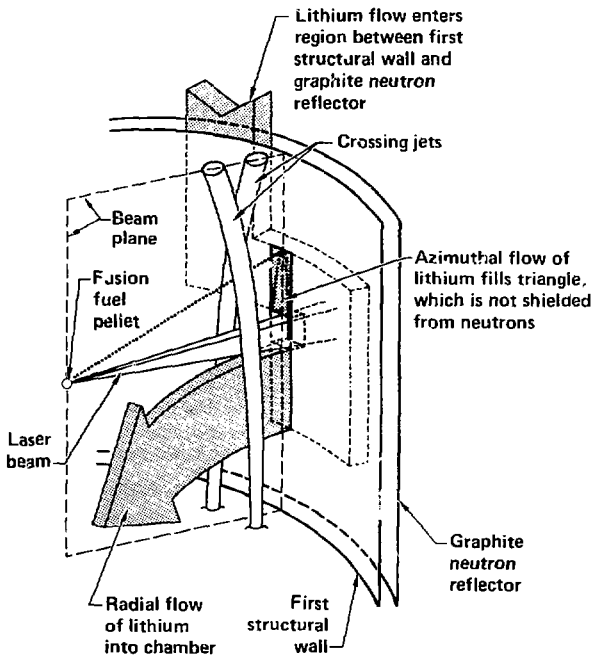

Figure 9. Beam aperture formed by flowing liquid metal. No structural metal is exposed directly to the fusion neutrons.

aperture, which is formed by the flowing liquid metal. The cross section of the cluster of laser beams is a vertically oriented rectangle. Each of the two opposing beams is projected to the fuel pellet from a 6- by 2-m mirror array located 60 m away.

2.4.4 Condensation and Reestablishment of the Liquid-Metal Jet Array

Determination of the HYLIFE repetition rate was governed primarily by two constraints: the reestablishment time of the liquid-metal wall and the reestablishment of the chamber vacuum. With a 4.6-m head of Li, it takes 0.64 s for the liquid metal to travel from the bottom of the nozzle plate to the bottom of the chamber. With this time consideration, the repetition rate would be 1.5 Hz.

The chamber vacuum can be reestablished using external vacuum pumps or by cooling and recondensation within the chamber. Attempting to remove the several kilograms of vaporized Li from the chamber in 0.6 s by pumping would require more pumps than are practical. However, the HYLIFE chamber environment, with its enormous liquid surface area, is itself a large vacuum pump.

The ablated gas is still very hot, even after it has vented through the liquid-metal jet array, and it cannot condense until it cools to nearly the liquid temperature. This post-venting cooling period dominates the vacuum reestablishment time. The cooling rate depends on the liquid surface area. This surface area is estimated to increase by two orders of magnitude by jet fragmentation (to 2 mm in diameter for the inner jet and to 1.3 cm in diameter for the outer jets), then to decrease due to the fragments rejoining (caused by the higher velocities of the inner fragments), and then to increase again while the recompacted annulus coasts to the wall (since the diverging geometry causes cavitation).[47]

We investigated the cooling rate for several surface areas. With a surface area equal to that with 10-cm-diam cylindrical jets (assuming no disassembly of the jets), we estimated a cooling time of approximately 500 ms, the majority of which was the time period after the gas temperature fell to approximately 0.5 eV (Ref. 48). With 2.5-cm-diam spherical droplets, we estimated a cooling time of approximately 50 ms.[19] Because our maximum estimated fragment size is 1.3 cm, actual cooling times in HYLIFE should be less than 50 ms. Cooling times of 500 ms are permissible with the chamber repetition rate of 1.5 Hz.

2.5 Structural Design

One of our most difficult problems in developing HYLIFE was to design the first structural surfaces—the nozzle plate and the FSW.[49-51] In this section, we review the stresses on the nozzle plate and FSW caused by the various loads, the design criteria used, and the material issues and research performed in support of the HYLIFE structural design.

2.5.1 Nozzle Plate

The final HYLIFE nozzle-plate design (Fig. 10) uses 2-1/4 Cr–1 Mo ferritic steel, with rectangular orifices made from welded angle plates, to produce rectangular jets and vertical flow.[52-54] The nozzle plate also features a large hole at the center to allow for the expansion of the liquid-metal vapor. The first row of jets is actually a weir flow that breaks up above the midplane, allowing passage of the driver beams. The weir flow also provides x-ray and debris protection for the inner edge of the nozzle plate. The plate itself is clamped in place, the lack of welds or bolts allowing easy replacement. The rectangular hole construction produces a higher liquid-packing fraction than round holes.

We used a finite element program to examine the loads on the nozzle plate resulting from (1) the static liquid-metal head on the nozzle plate, (2) the steady drag of the liquid metal flowing through the nozzles, (3) the dynamic loads due to neutron-energy deposition in the liquid-metal pool, and (4) the time-dependent pressure from the vapor ablated from the liquid-metal jet array by the fusion pulses.

The peak static stress in a 0.5-m-thick nozzle plate is about 60 MPa, and the peak dynamic stress is about 10 MPa.[54-57] We used a crack-propagation analysis[58] to show that at these stresses initial crack lengths of about 20 mm will not propagate; larger cracks can easily be detected by ultrasonic equipment. The natural frequency for this nozzle plate is about 60 Hz.[52]

2.5.2 First Structural Wall

The FSW isolates the vacuum-vessel wall from the pulsed effects of the fusion energy. The FSW must resist loads from liquid metal that is vaporized by the x rays and from liquid metal fragments generated by the sudden neutron-energy deposition. We determined the maximum radial displacement of the FSW by coupling the time-varying pressure load from these sources

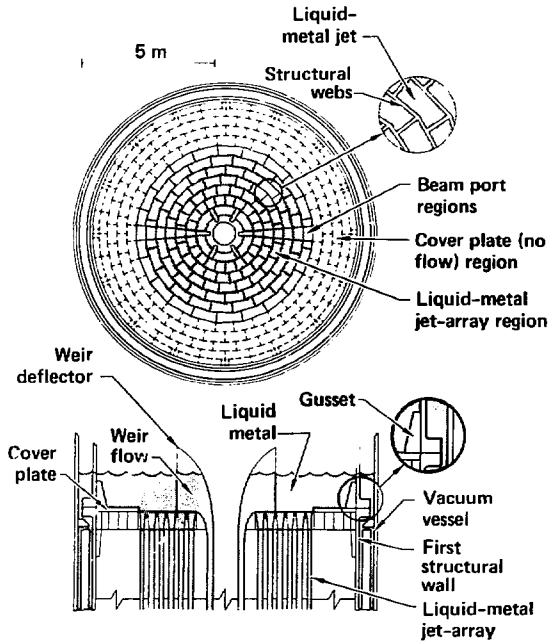

Figure 10. HYLIFE nozzle plate. The first row of jets is actually a weir flow that breaks up above the midplane to allow passage of the driver beams. The weir flow also provides x-ray and debris protection for the inner edge of the nozzle plate.

with the equation of motion of the FSW. This displacement determines the maximum dynamic stress in the wall.[26,28,59]

The FSW experiences a steady stress caused by the essentially steady-state temperature distribution through its thickness. This temperature distribution is caused by volumetric heat generated from neutrons and gamma rays that are absorbed in the FSW, coupled with the surface cooling from lithium flowing on both sides of the FSW.[59,60] The pulsed nature of the volumetric energy deposition in the FSW causes dynamic variation in the thermal stress, but the variation is small when compared with either the average thermal stress or the gas or liquid impact stresses. Our calculated steady and pulsed stresses were within the levels allowed under the ASME Pressure Vessel Code.[61-64]

Our design work on the FSW emphasized the wall's response to the liquid-metal impact. We analyzed the response of one jet-array design to energy deposition from one fusion-pulse level, and then scaled the results for the liquid-metal impact to different chamber and jet-array geometries as well as different fusion yields. We coupled our findings with the thermal stress analysis and design criteria to obtain an FSW design map (Fig. 11).[25] Our results show that the impact stress in the FSW decreases with increasing wall thickness. The thermal stress in the FSW, however, increases with increasing wall thickness.

In order to meet the requirements of the ASME Pressure Vessel Code, we needed to satisfy two conditions. The first condition required the total stress in the FSW to be less than the yield strength of the wall material (at its peak temperature). The second condition required the pulsed stresses to be less than half the fatigue strength of the wall material (at its peak temperature). Both conditions were evaluated as a function of wall

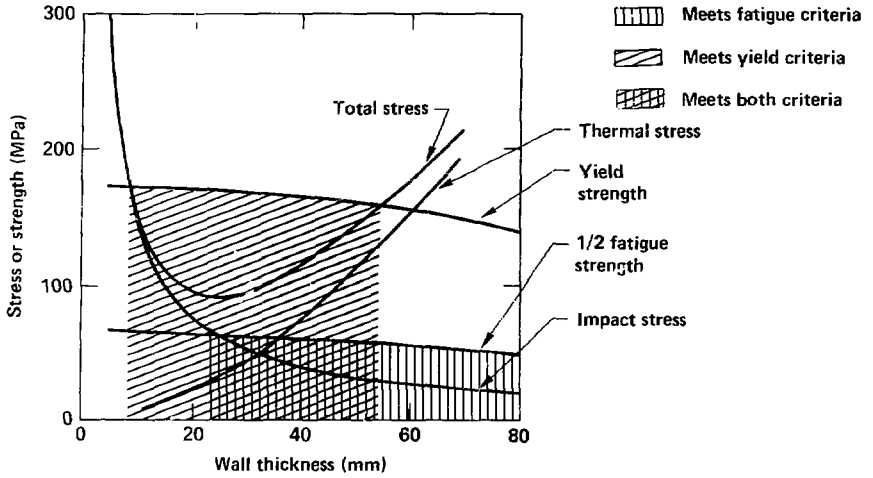

Figure 11. Pulsed and steady stresses vs wall thickness and the limiting levels under the ASME code. *Wall thicknesses in the 25- to 55-mm range satisfy both ASME criteria: total stress less than* yield strength and pulsed stress less than one-half the fatigue strength. This figure is based on an early HYLIFE design with a 2700-MJ yield. The jet array in this early design has a 0.75-m inner radius, is 1.0 m thick, and has a midplane packing fraction of 50%.

th[illegible]ness and jet-array inner radius. A range of [illegible]inations of fusion yield (or pulse rate), wall [illegible]ness, array radius, array-packing fraction, [illegible] array thickness satisfied both conditions and [illegible]t the ASME Code design criteria. (See Fig. 11.) The combination selected for the final design minimized the liquid-metal flow rate, pumping power, and inventory while satisfying the ASME Code.

The minimum effective liquid-metal-array thickness in the final design (74 cm) was specified to permit a 30-year wall lifetime at a 70% capacity factor (165-dpa radiation damage limit). To minimize the liquid-metal flow rate and, hence, the pumping-power requirements for a given fusion power and wall radius, we chose our design point where both the effective array thickness (74 cm) and the array inner radius were minimized.[25] Our results show that for these jet-array parameters, an FSW thickness of between 35 and 40 mm of 2-1/4 Cr-1 Mo steel will meet the ASME criteria. The flow rate is minimized for 1800-MJ, 1.5-Hz pulses, and the array midplane packing fraction is 57% in the final design.

2.5.3 Materials Considerations

The deposition of intense pulses of radiation energy in structural material demands unique requirements for ICF. The issues we considered included the ability of the material to withstand the simultaneous mechanical and thermal stresses, radiation damage, and liquid-metal corrosion. These issues are discussed in more detail in Refs. 65–67.

We evaluated the compatibility of structural materials for HYLIFE with the liquid-metal (lithium) jet array. We considered both austenitic and ferritic steels for the first structural surfaces, and chose 2-1/4 Cr-1 Mo ferritic steel over the 300-series austenitic stainless steels. The austenitic steels are stronger than the ferritic steels, but the liquid lithium leaches out the nickel from the austenitic steel, causing corrosion rates to increase with the nickel content.[4,68] Since the ferritic steels

are nickel-free, they resist liquid-lithium corrosion; they also produce fewer radioisotopes and damaging (n,α) reactions.[4]

While the ASME Pressure Vessel Code does not presently permit high-temperature use of 2-1/4 Cr-1 Mo steel, there is a large body of data available that allows the design of the structure using the methodology[61-64,69] of the code. Oak Ridge National Laboratory[70] obtained fatigue data and presented it in the form required by the ASME code.[71] Much of the other mechanical property data is included in the *Nuclear System Materials Handbook*.[72] The effects of liquid-metal corrosion and the mechanical properties of the 2-1/4 Cr-1 Mo steel for various heat treatments, which were studied at the Colorado School of Mines, are discussed below.[73]

Early experiments using small samples of 2-1/4 Cr-1 Mo steel (with unstabilized carbides) in static liquid lithium confirmed that the ferritic steel showed good corrosion resistance at approximately 750 K, but the corrosion rate increased dramatically if the nitrogen concentration in the lithium increased over 500 appm (Ref. 4). The corrosion rate of the bulk of the 2-1/4 Cr-1 Mo steel was less than that of 304 stainless steel; however, significant grain-boundary penetration was observed in the heat-affected zone of welded pieces of 2-1/4 Cr-1 Mo steel. Because of these observations, we studied the effect of stabilizing the carbides in 2-1/4 Cr-1 Mo steel by either adding niobium, or by post-weld heat treatment. We used a liquid composition of 17.6 wt% lead (0.71 at.%) in lithium. The lead impurity was added to simulate possible debris from fusion fuel pellets. The niobium-stabilized, 2-1/4 Cr-1 Mo-steel weld specimens were found to be resistant to intergranular attack even when no post-weld heat treatment was applied. The unstabilized 2-1/4 Cr-1 Mo heat-affected zones showed improved resistance to lithium corrosion when the specimens were given a post-weld heat treatment that converted the Fe_3C to more stable metal carbides.[74-77]

Further experiments were conducted using 2-1/4 Cr-1 Mo ferritic-steel specimens that had been heat-treated to duplicate the microstructure found in the heat-affected zone of previous experiments. The lead concentration of the liquid lead-lithium was varied from 0 to 99.3 wt% in a series of static tests, and from 0 to 17.6 wt% for flowing liquid. Again, we found post-weld heat treatment to be very effective in preventing intergranular penetration by the liquid metals. Also, the penetration of the 17.6 wt% lead in lithium was independent of liquid velocity up to a value of 0.3 m/s.[78-81]

Liquid-metal-induced embrittlement of 2-1/4 Cr-1 Mo steel is currently under investigation. Test specimens that had been heat-treated to simulate the heat-affected zone of a weldment were severely embrittled by 17.6 wt% lead in lithium at temperatures up to 800 K. An intensive temper reduced the embrittlement susceptibility of these specimens, but it also reduced the strength and low-temperature ductility of the base material.[82] We also investigated the effect of embrittlement by pure lead and pure lithium. Each liquid caused liquid-metal-induced embrittlement in the simulated heat-affected zone of the 2-1/4 Cr-1 Mo steel in a 100-K temperature range just above the melting point of the liquid metal. Changing the post-weld heat treatment (that converts the Fe_3C to more stable metal carbides) from 1010 K for 10 hours to 970 K for 120 hours was found to reduce embrittlement.[83]

We concluded that 2-1/4 Cr-1 Mo ferritic steel is an acceptable material for our fusion application. Further stabilization of carbides by either additional Nb or post-weld heat treatment of heat-affected zones reduces grain-boundary penetration when ferritic steel is exposed to liquid lithium or lead-lithium alloy. Increasing the tempering time also reduces liquid-metal-induced embrittlement to acceptable levels.

3. Supporting Systems

In this section, we summarize the consideration that we gave to five areas of supporting systems: driver options, protection of final optics, fuel-pellet injection, vacuum system requirements, and tritium extraction.

3.1 Driver Options

Three drivers were considered for HYLIFE: lasers, heavy ion beams, and light ion beams. For

our conceptual baseline, we selected the short-wavelength laser (SWL). In our calculations, we assumed 5% laser efficiency and 4.5 MJ of laser energy, driving a fuel pellet to a gain of 400. (A 1-GWe power plant would require a 1.5-Hz repetition rate.)

Which type of SWL should be used for the HYLIFE concept is still subject to debate (e.g., solid state, KrF, or free electron laser). Experiments have shown that the laser wavelength should be less than 0.5 μm to heat the fuel pellet efficiently and to maintain a low fuel-pellet preheat from hot electrons. Solid-state (Nd:glass) lasers that can be shifted to the necessary frequency may be able to achieve the 1.5-Hz repetition rate if the lasing medium is cooled with high-pressure helium. The resulting efficiencies could, in principle, exceed 10%.[84]

A heavy-ion-beam driver could achieve about 25% efficiency at high repetition rates. Although a heavy ion beam would require no change to the HYLIFE reaction-chamber geometry, it would require a lower vacuum pressure in order to propagate the beam to the fuel pellet.[5,85] Heavy ion beams need a vacuum pressure of less than 10^{-2} or 10^{-1} Pa ($\sim 10^{-4}$ and $\sim 10^{-3}$ Torr) for ballistic beam propagation. For HYLIFE, either the temperature of the pure lithium would have to be reduced to between 670 and 720 K, or the lead-lithium eutectic (83% Pb, 17% Li) would have to be used at 770 K to prevent the liquid-metal vapor pressure from exceeding these limits. Figure 12 shows the vapor pressure of liquid metals as a function of temperature. The corresponding limit for an SWL driver is between 10 and 100 Pa ($\sim 10^{-1}$ to ~ 1 Torr).

Lowering the liquid-metal temperature reduces the thermal/electric conversion efficiency[86]; using lead-lithium at 770 K keeps the same thermal efficiency but requires greater pumping power and a larger heat exchanger (due to the different thermal conductivities of lithium and lead-lithium). It should also be noted that it may be possible to dispense with the intermediate heat-exchange circuit in the lead-lithium design. However, in this event, there is concern that adequate tritium containment may be difficult to achieve.

Table 5 summarizes the energy balances of three conceptual power plants: the laser-driven, pure-lithium baseline design; a heavy-ion-driven

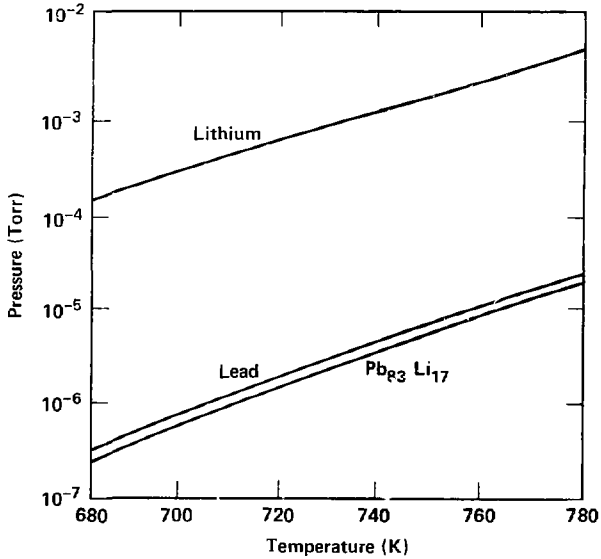

Figure 12. Vapor pressure of lithium, lead, and the lead-lithium eutectic as a function of temperature.

Table 5. Energy balance of three HYLIFE power plant designs: Baseline = laser-driven, pure lithium at 770 K; HI1 = heavy-ion-driven, pure lithium at 670 K; HI2 = heavy-ion-driven, lead-lithium at 770 K.

	Baseline	HI1	HI2
Driver pulse energy (MJ)	4.5	4.5	4.5
Driver efficiency (%)	5	25	25
Pulse energy (MJ)	1800	1800	1800
Fusion power (MW)	2700	2700	2700
Fusion chamber output (MW)	3177	3177	3177
Pump heating (MW_t)	39	39	244
Gross thermal energy (MW_t)	3216	3216	3532
Thermal to electric efficiency (%)	39	34	39
Gross electric power (MW_e)	1254	1093	1377
Driver power (MW_e)	90	18	18
Auxiliary power (MW_e)	96	96	359
Total in-plant electricity (MW_e)	186	114	377
Net electricity (MW_e)	1068	979	1000
Net efficiency* (%)	33.6	30.8	30.4

*Net electric power/fusion chamber output power.

lithium design; and a heavy-ion-driven, lead-lithium design. The net electrical efficiency of the laser-driven, pure-lithium baseline is the best, although the differences among the three are not large. We conclude that the HYLIFE reaction chamber concept is adaptable to either a laser or a heavy-ion-beam driver.

3.2 Design and Protection of Final Optics

Our conceptual laser driver is housed in a nonnuclear building that is separate from the reactor containment building. This reduces building costs and construction time and provides better laser access and maintainability. The two laser beams travel to the reactor through underground pipes that link the two buildings. Each beam enters the containment building through a separate window (Fig. 13) and is line-focused through its own small slot in its own fast-acting safety valve. The valve provides secondary containment protection in case of window failure. Fixed, off-axis, parabolic focusing mirrors direct each beam onto a set of flat mirrors, which may be mounted on a carousel accommodating several replacement flat-mirror sets to reduce maintenance down-time. The final flat mirrors are located at the turning point of the beam tubes in a direct pathway to the fusion pulse (Fig. 13) and are exposed to neutrons from the fusion reactions.

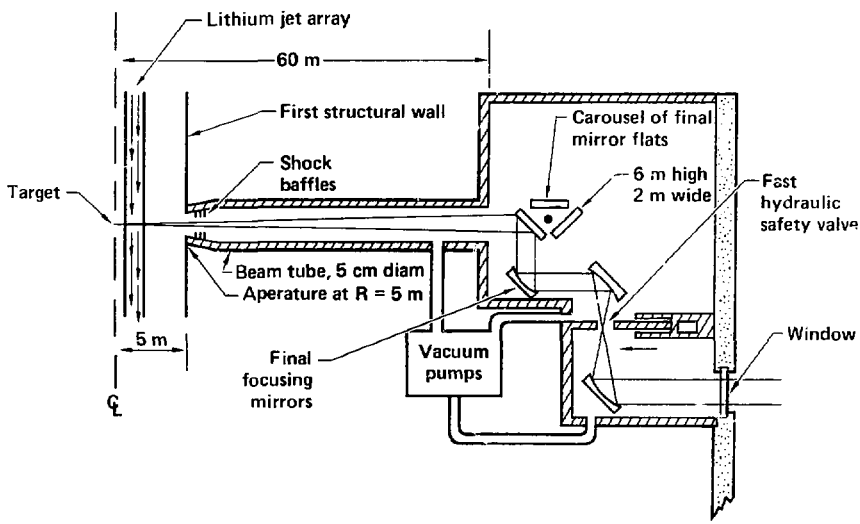

Figure 13. Schematic of the final focusing system. The expensive parabolic focusing mirrors are not in the target's line of sight, and therefore should survive for the life of the plant.

To protect the flat mirrors from x rays and debris, we considered small solid angles with high *f*-number optics, magnetic fields, transparent films, rotating shutters, gas barriers, gas refractors, and liquid-metal mirrors.[87] We finally chose a combination of high *f*-number optics and a gas barrier.

The two sets of final mirrors are located 60 m from the reaction chamber and have a total area of 23 m^2 (assuming an optical damage threshold of 20 J/cm^2). If the mirrors were closer to the chamber, they would subtend a large solid angle, and energy losses out of the chamber would be greater. The solid angle with the mirrors 60 m from the chamber is only 5×10^{-4} sr. The neutron exposure at this distance is 0.042 MW/m^2 (Ref. 88). Testing will be required to determine the damage to the final mirrors at this flux, but we estimate the mirrors will have a 3-year lifetime.

The most effective system we have found to prevent x rays and debris from contacting the final optic assembly uses a recirculating pump to inject a gas with a relatively high atomic number (such as xenon) at the optical surface. The photoelectric interactions in the gas stop the x rays, and collisions between the particles thermalize the fuel-pellet debris. Intermediate stations pump the gas out of the tube, preventing it from reaching areas near the chamber center or the entrance slot (safety valve) where the high-beam intensity could cause gas breakdown.

In Fig. 14, we show the mean free path of x rays as a function of their energy in one atmosphere of xenon gas. (We use data from the LLNL

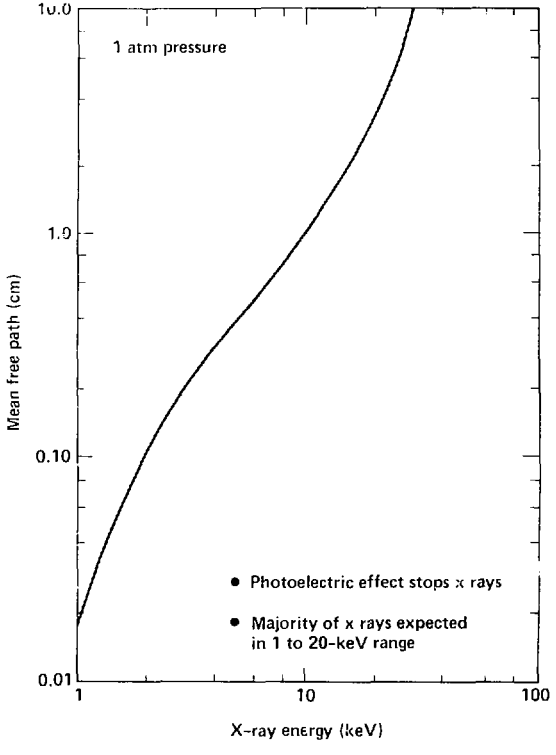

Figure 14. X-ray stopping power of xenon gas.

photon cross-section library.[89]) A total of 210 Pa·m of xenon will provide one attenuation mean free path for 3-keV x rays. To reduce the x-ray intensity by a factor of 100, we must provide 4.6 mean free paths of gas, or 970 Pa·m of xenon. A 10-m section of beam tube containing 130-Pa (1-Torr) xenon should be able to absorb the radiation over enough distance to prevent the generation and transmission of shock waves. An additional benefit of this gas system is that the counter-flowing gas isolates the cooled mirror from the hot lithium vapor, which might otherwise tend to condense on the optical surface.

Depending on the final damage limit obtained and the final wavelength selected, the final optics could be either coated or uncoated metal mirrors. The mirrors are heated by neutrons and absorbed laser radiation. We calculated an optical heat load of 0.3 W/cm^2—a level that poses no serious problem because conduction cooling can prevent distortion of the mirror surface.[87] The neutron-heating contribution is perhaps slightly higher.

We have identified three mechanisms that could lead to shortened lifetimes for the final (flat) metal mirrors:

- An increase in optical absorption by reduction of electron conductivity in a damaged lattice (uncoated mirror).
- An increase in optical distortion caused by swelling from (n,α) helium-production reactions (both uncoated and coated).
- A distortion and decreased damage threshold of high-reflectance coatings.

Presently, we have no information on the swelling of copper or other substrate materials at 14 MeV. Therefore, for our calculations, we have used data on stainless steel. At a distance of 60 m, we estimate a lifetime of 1 to 4 years.

3.3 Fuel-Pellet Injection

The pulsed operation of HYLIFE requires precise timing. The injection of the cryogenic fuel pellets must correspond to the chamber repetition rate. If the blanket material is liquid lithium, there must be enough time between the injection of fuel pellets to allow any vaporized lithium to condense.

The frozen DT fuel pellet must be injected at a speed that keeps it from being heated above its 19.8-K triple point. Exposed surfaces of DT must be kept below about 14 K to reduce surface migration (by sublimation and redeposition) and consequent loss of symmetry of the pellet. The typical HYLIFE chamber temperature is ~770 K. Our heat-transfer calculations show that multiple-layered fuel pellets must be injected at a speed greater than 300 m/s so that their exposure to the hot chamber is less than 18 ms.[90,91]

Figure 15 illustrates the phases in the life of a HYLIFE fuel pellet. After manufacture, the fuel pellet is stored for a short time in a pool or stream of liquid helium at 4.2 K. The fuel pellet is then encapsulated in a sabot and accelerated to injection speeds. The sabot would most likely be removed just prior to injection into the chamber; however, it could be manufactured of frozen lithium and injected into the chamber along with the fuel pellet. In the latter case, the sabot could act as a pre-pellet to clear any lithium droplets in the pellet's path. Finally, when the pellet is approximately 1 mm from the chamber center, the laser is

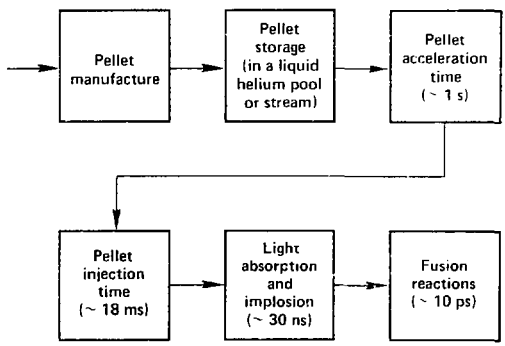

Figure 15. Phases in the life of an ICF fuel pellet.

triggered so that the beams will intercept the pellet at exactly the chamber center. The laser light is absorbed, the pellet is imploded, and the fusion reactions occur.

3.4. Vacuum System

We based the HYLIFE vacuum system on a cavity-equilibrium temperature of 770 K, using the design criteria listed in Table 6.[92] Two levels of hydrogen were evaluated to allow for uncertainty in the amount of hydrogen that might diffuse into the lithium from the water loop, via the Na intermediate loop. During the first 250 ms, the vacuum pumps are protected from high pressure in the cavity by a shutter valve. Results of the analysis for an initial pressure of 0.13 Pa (10^{-3} Torr), excluding lithium, showed that the total effective pumping speed was 755 and 2000 m^3/s, depending on whether the low or high hydrogen values were used. We developed a large, yet satisfactory, vacuum pumping system that can be used with a 0.13-Pa (10^{-3} Torr) chamber pressure appropriate for heavy-ion-beam drivers. (See Table 7.) A smaller vacuum system is feasible if we use a laser driver, which requires only 13 Pa (10^{-1}) chamber pressure instead of the heavy-ion-beam driver.

Table 6. Design criteria for the HYLIFE vacuum system.

Gas	Generation g/pulse	Partial pressure increase, Pa (Torr)
Deuterium	0.0074	0.0278 (2.09×10^{-4})
Tritium	0.0196	0.0491 (3.69×10^{-4})
Helium	0.0176	0.0664 (4.99×10^{-4})
Hydrogen	0.0054 or 0.152	0.0406 (3.05×10^{-4}) or 1.14 (8.6×10^{-3})
Total	0.05 or 0.195	—
Initial pressure conditions		
Lithium	0.48 Pa (3.6×10^{-3} Torr)	
Other gas	0.13 Pa (10^{-3} Torr)	

3.5 Tritium Extraction

Tritium is removed from the liquid lithium using a molten-salt extraction process. Studies by Calaway and Maroni at Argonne National Laboratory[93,94] indicate that the molten-salt extraction process, based on LiF-LiCl-LiBr (22-31-47 mol%), is an attractive technique for recovering tritium

Table 7. **Vacuum pumping system definition for selected design points.**

Parameters	Low hydrogen	High hydrogen
Evolved mass per pulse, g	0.05	0.20
Average molecular wt	4.1	2.3
Pressure rise, Pa (Torr)	0.19 (1.4×10^{-3})	1.3 (9.7×10^{-3})
Initial pressure (excluding lithium), Pa (Torr)	0.13 (10^{-3})	0.13 (10^{-3})
Effective pumping speed (1270 K), cfm (m^3/s)	1.6×10^6 (755)	4.4×10^6 (2000)
No. of pumping ducts (assumed)	40	40
Duct configuration	3 ft diam × 10 ft (0.9 m diam × 3 m)	3 ft diam × 10 ft (0.9 m diam × 3 m)
Required pump speed/duct at 295 K, cfm (m^3/s)	25 000 (12)	62 000 (29)
Assumed pumps/duct	1 × 25 000 cfm	2 × 30 000 cfm
Total number of pumps	40 at 25 000 cfm	80 at 30 000 cfm
Duct conductance/pump speed	3.4	6.3

from liquid-lithium fusion-reactor blankets. By using this processing method, we can maintain tritium levels in the lithium blanket at concentrations less than 1 wppm.

The molten-salt extraction process is illustrated in Fig. 16. A side stream of lithium from the fusion chamber contacts the LiF-LiCl-LiBr salt, one of the few materials with a higher affinity for tritium than lithium. The tritium is removed from the lithium and remains with the salt. The two immiscible liquids are then separated: the lithium returns to the fusion chamber, and the molten salt is circulated to an electrolytic processing tank. The tritium recovered in the electrolysis process is returned to the fuel-pellet factory.

The molten-salt extraction process appears to be applicable throughout the entire range of desired tritium concentrations. No limiting behavior in the electrochemical processing technique[94] was found down to an experimental limit of 0.06 wppm of tritium in lithium. The molten-salt extraction process is a modular system, with relatively small units connected in parallel. The processing requirements increase linearly with decreasing tritium concentration.

For HYLIFE, we propose maintaining the tritium concentration at ~1 wppm or a total tritium inventory of ~1 kg in the liquid lithium. A lithium flow rate of 0.12 m^3/s is required through the extraction system.[95] This is less than 1% of the flow rate required for heat removal and less than 0.1% of the total lithium flow in the HYLIFE jet-array circulation loops.

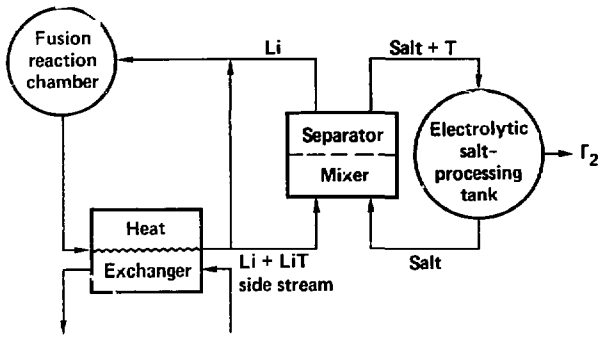

Figure 16. Molten-salt, tritium-extraction process to remove tritium from liquid lithium.

4. Primary Steam-Supply System and Balance of Plant

This section focuses primarily on the transfer of energy from the liquid-lithium primary coolant to the turbine generators, where electricity is produced. We discuss the heat transport system and its components, as well as the thermodynamic cycles we selected.

The heat transport system for the HYLIFE reactor power plant is made up of three subsystems.[96,97] The first subsystem (primary loops) circulates the lithium from the fusion chamber to four intermediate heat exchangers (IHX). The second subsystem (intermediate loops) uses sodium to transport the heat energy from the 4 IHXs to 12 steam generators. The third subsystem (secondary loops) uses water/steam loops to transport the thermal energy from the steam generators to the turbine generators which convert heat into mechanical and then electrical energy.

The primary loops consist of pumps that circulate the lithium through the HYLIFE chamber

as well as through the heat transfer system. About 90% of the primary lithium flow is returned directly to the chamber; the remainder of the flow is transported to the IHXs for energy extraction.

The final design (Fig. 17) uses eleven 7.8 m^3/s pumps to recirculate the primary liquid-metal flow from the lower chamber outlet back to the upper inlets. Two additional pumps each transport 4.9 m^3/s to two IHXs each, and return the cool lithium to the chamber outlet. This arrangement sets all 13 pump heads at roughly equal levels, easing maintenance and increasing safety. To minimize the effects of pressure pulses in the liquid lithium, 35%-efficient electromagnetic pumps were specified. Later studies indicate that efficiencies of greater than 50% can be achieved by proper pump design.[98,99]

The heat energy in the lithium loops is transferred through four IHXs to the sodium loops. The intermediate sodium loops are designed to eliminate the possibility of an exothermic reaction between the liquid lithium, which contains radioactive materials (activated corrosion products, fuel-pellet debris, and tritium), and the water in the steam loops. The only radioactive contaminant in the sodium loops is tritium, which diffuses from the lithium through the walls of the IHX. This tritium can be cold-trapped to a concentration of less than 0.13 wppm in the circulating sodium[100]; thus, the tritium inventory in the sodium is an order of magnitude lower than the tritium inventory in the lithium.

The IHXs are of two-pass, shell-and-tube, counter-flow construction. They are, like the piping in both the lithium and sodium loops, made of 2-1/4 Cr-1 Mo steel. The IHXs are mounted vertically in the reactor building, each handling about 800 MW_t. The two sodium pumps are located on the return side, between the IHXs and the steam generators. Each handles about 4.5 m^3/s of sodium.

We have investigated two steam generator arrangements. The first arrangement uses three 268-MW_t shell-and-tube steam generators per 800-MW_t IHX. Each of the 12 steam generators produces 730-K, 15.8 MPa superheated steam. The second arrangement uses one steam generator and one superheater per IHX.[101,102]

Other equipment includes liquid-metal storage systems, the liquid-metal cover-gas processing system, hot cells, the low-level-waste handling system, diesel generators for emergency auxiliary power, and other systems necessary for the support of an electric power plant. Details of these systems are presented in separate reports.[102,103]

The primary steam-supply system and balance of plant can be built using today's technology—that is, all components except for the liquid-metal pumps, turbines, and steam generators.[97] The designs used in our research for these components are only modest extrapolations of technology.

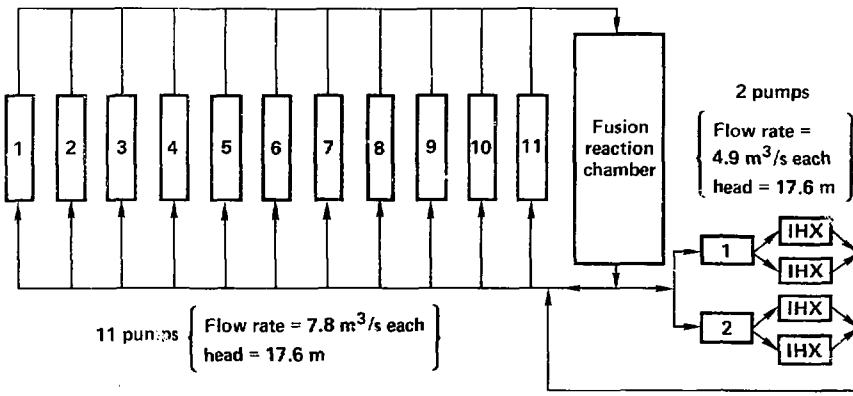

Figure 17. Primary steam-supply system. All 13 pumps have subatmospheric outlet pressures, which minimizes potential lithium leakage.

5. Safety and Environmental Protection

From its inception, the HYLIFE reactor study was conducted with safety as a principal goal. In order to reduce radioactivity and increase nuclear safety, we selected 2-1/4 Cr-1 Mo, a relatively low-activating steel, to construct the reactor; a liquid-metal wall to protect the steel; and simple assembly procedures. We also used inert gas to fill rooms where fire could cause a hazard. Both fire safety and nuclear safety analyses were performed.

5.1 Fire Safety

For an accident with the HYLIFE reactor to endanger the general public, the accident must involve a large-scale reaction of molten lithium with air, water, or concrete. Furthermore, the reaction heat must be coupled with radioactive components, either directly in the flame or indirectly via heated gas. Several passive features intrinsic to the HYLIFE design minimize the possibilities of these chemical reactions and heat transfer.

First, the HYLIFE reactor room, surrounded by other rooms and the crane loft, is filled with inert gas to prevent contact between lithium and air in case of a pipe break. In the event of a large air leak into the reactor room, the lithium can be drained in minutes. (Even in such a case, lithium combustion could not occur for hours.) After removal of the circulating liquid-lithium wall coolant, the rather low level of wall afterheat can be removed by passive thermal radiation. And since the FSW is a low-tolerance insert in the vacuum vessel, it can easily be repaired or replaced in the event of damage from overheating.

Second, the reactor building is segmented, no water or steam components exist in the reactor room, and all concrete is steel-lined. The lithium-loop peak pressure is subatmospheric, which means that small leaks would be inward. In the case of a large lithium leak, the lithium would fall on a sloped floor and flow into tall, narrow, drain tanks. The tanks contain iron balls to rapidly cool the liquid metal to less combustible temperatures and hollow graphite microspheres that float on the surface of the liquid to prevent contact between the liquid metal and the air, in the event of a simultaneous liquid-metal spill and air leak. These precautions would virtually eliminate the possibility of large-scale liquid lithium fires and vaporization of the activated FSW.

Although the intrinsic design features of HYLIFE minimize the possibility of large-scale lithium fires, knowledge of the reaction rates and energy releases is essential to conducting a proper safety analysis. Many misleading safety studies begin with the assumption that spilled lithium burns completely within a short time. Experiments have shown that this assumption is unrealistic.[104] A long contact time with little heat loss is necessary before a vigorous lithium-concrete reaction could begin. Thus, in a HYLIFE reactor spill, only a small fraction of the lithium would burn, and that combustion would occur at a safe distance from radioactive structural materials.

5.2 Nuclear Safety

Our earliest nuclear safety studies[105-108] compared the activity and gamma emission from 2-1/4 Cr-1 Mo ferritic steel with that from stainless steel walls. The ferritic steel had half the gamma emission rate of the stainless steel just one day after shutdown, and at 10 years after shutdown its rate was 50 times lower. In addition, the liquid-metal-wall protection reduced the activation for both ferritic and stainless steels. At shutdown, the stainless steel activity per GW_e for HYLIFE is 60 times lower than for the UWMAK-1 tokamak.

Calculated dose rates inside and outside the HYLIFE chamber show that hands-on maintenance of the chamber is not possible and that a 2-m-thick concrete shield would be necessary to reduce the shutdown dose from the FSW to negligible levels (0.1 μR/hr). The activation of corrosion products and fuel-pellet debris was also considered, but this was not significant when compared to the structural activation.

Later activation studies[109-118] quantified the activation of various steels in both HYLIFE and magnetic fusion geometries in terms of curies, afterheat (decay heat), inhalation-biological-hazard potential, ingestion-biological-hazard potential, chemical-ingestion-biological-hazard potential, waste disposal, and surface dose rate. The HYLIFE geometry provided an order of magnitude reduction in activity (to 300 MCi at shutdown) compared with magnetic fusion geometries. The HYLIFE afterheat (2 MW) was found to be low enough that radiation cooling of the FSW is possible. No emergency wall-cooling system is

required, in contrast to both fission and magnetic fusion. The inhalation-biological hazard-potential for HYLIFE (5×10^6 km^3) is an order of magnitude less than that for a magnetic fusion wall, but the level is still so high that accidental release fractions of less than 10^{-6} are required for safety; hence, the release fraction rather than the source magnitude will dominate the hazard. The surface dose rates of all steel first walls were very high ($\sim 10^5$ *R/h*); *therefore, remote maintenance will* be required.

Waste disposal studies[118] revealed that disposal in shallow land-burial sites will be feasible if certain impurities (niobium) are minimized in the original steel. In some cases, dilution by one to two orders of magnitude in volume will be required; this dilution material is already available from the lower-activated blanket and shield components, which must also be discarded. The advantage of lower activation in the HYLIFE wall (due to the liquid protection) was offset by the longer irradiation time (30 years compared to ~5 years in a magnetic fusion reactor) because the disposal limits are in terms of activity per unit volume. However, once the limits are met, only one HYLIFE wall must be discarded—compared to approximately six magnetic fusion walls of equivalent hazard.

The final nuclear safety issue concerns tritium. *Tritium is much less hazardous than other* radionuclides, but it is also difficult to contain. Because tritium is extremely soluble in lithium, tritium leakage from the lithium into the sodium will be low (~1 kCi/d) compared to the 10-MCi/d tritium-circulation rate.[100,119] A combination of diffusion barriers, sodium cold-trapping, and water-loop processing is expected to reduce tritium emission from the power plant to the 10 to 100-Ci/d level.

6. Costs

In this section, we review the estimated capital cost of the HYLIFE power plant and the resulting cost of electricity. As a point of reference, the costs for the HYLIFE reactor are compared with those for current light-water fission reactors (LWRs).

Table 8 gives a breakdown of the total direct capital costs (TDC) in 1983 dollars for both single- and dual-unit plants. The single-unit plant consists of a laser driver, a fuel-pellet factory, and a reactor that produces about 1 GWe of electricity. The dual-unit plant produces about 2 GWe and has two full-size reactors. A single driver serves both reactors by switching beams from one to the other. As such, the driver in the dual-unit plant operates at twice the pulse repetition rate of the single-unit plant. Likewise, the fuel-pellet factory for the dual-unit plant must produce fuel pellets at twice the rate of the single-unit factory.

The costs for the single-unit HYLIFE reactor were estimated by Bechtel National Corporation and reported in 1980 dollars.[120] To allow us to compare the most recently published LWR costs,[121] we escalated the costs from Ref. 122 by 32%, converting them to 1983 dollars. We reduced the reactor plant-equipment cost given in Ref. 120 by $55 million (1983 dollars) to reflect the lower lithium-flow rate in the final design (96 m^3/s compared with 129 m^3/s). The TDC for a dual-unit reactor is less than twice the cost for the single-unit reactor. The scaling between the single- and dual-unit plants is based on methods used by Bechtel National Corporation.[122]

Table 8. Total direct capital costs (TDC) for single-unit (1-GWe) plants and dual-unit (2-GWe) plants (1983 dollars). The cost of the dual-unit reactor is only about 175% of the cost of a single-unit reactor. Also, a single laser is used to drive both reactors in the dual-unit plant.

	Single-unit ($ million)	Dual-unit ($ million)
HYLIFE reactor		
Structures and site facilities	392	648
Reactor plant equipment	674	1202
Turbine plant equipment	230	438
Electric plant equipment	102	184
Misc. plant equipment	22	32
Subtotal	1420	2504
Laser	666	733
Fuel-pellet factory	100	150
Contingency (15%)	328	508
Total direct capital cost	2514	3895
Total direct capital cost per GWe	2489	1928

The costs of the laser driver and fuel-pellet factory are uncertain. The laser cost of $666 million is based on $200 million for 1 MJ and a

0.8-power scaling with beam energy (i.e., \$200 million × $E^{0.8}$, where E is the beam energy in MJ). Although we have not specified a particular type of laser, this cost is consistent with published cost estimates for KrF lasers.[123,124] The cost for advanced, solid-state lasers is unknown at this time. The additional cost incurred in doubling the laser-pulse repetition rate from 1.5 to 3.0 Hz to drive the dual-unit plant is taken to be 10% of the laser cost, or \$67 million.

The cost of the fuel-pellet factory that supports the 1.5-Hz, single-unit plant is assumed to be \$100 million (although no detailed study was done to arrive at this figure). Based on the scaling relationships reported in Refs. 125 and 126, doubling the fuel-pellet factory production rate in order to supply a dual-unit plant increases the fuel-pellet factory cost by about 50%. The TDC of the single-unit plant is \$2489 million/GWe, while the TDC of the dual-unit plant is \$1928 million/GWe.

Table 9 gives the total indirect cost (TIC), time-related costs, and the total capital cost (TCC) for both size plants. Also listed are the cost per net kW_e and the busbar cost of electricity. The fractions used to determine the TIC are based on guidelines given in Ref. 127. (In actual practice, TIC is a smaller fraction for the second unit than for the first.) The interest during construction is based on a constant dollar analysis (i.e., no escalation) using an 8-year construction period and a 5% real cost of money.[127]

The cost of electricity (COE) is equal to the total annual costs divided by the annual energy production. It is given by

$$\text{COE} = \frac{R(\text{TCC}) + f(\text{TDC} + \text{TIC})}{8760 P \alpha} \quad \$/kW_e h \tag{4}$$

where

TCC = total capital cost in dollars,
TDC = total direct capital cost in dollars,
TIC = total indirect capital cost in dollars,
R = 0.1 = fixed charge rate (yr^{-1})
f = 0.02 = operation and maintenance factor (yr^{-1}),
P = net electric power (kW_e),
α = 0.7 = capacity factor,
8760 = hours per year.

The cost of materials to make the fuel pellets is expected to be small and is therefore omitted. The 10% fixed charge rate is consistent with a constant dollar analysis. An annual cost equal to 2% of the sum of the TDC and the TIC is included for operation and maintenance costs.[127]

As indicated in Table 9, the single-unit plant produces electricity for 7.5¢/kW_eh. (This includes 6.4¢ for capital and 1.1¢ for operation and maintenance.) The dual-unit plant has significant cost advantages, producing electricity for 5.8¢/kW_eh, which includes 5.0¢ for capital and 0.8¢ for operation and maintenance.

To put these costs in perspective, we compare the COE for HYLIFE to the COE for an LWR (Fig. 18). Based on the most recent LWR cost information,[122] and using the same cost factors used for the HYLIFE plant (i.e., 15% for contingency, 35% for TIC, 17% for interest during construction, and the same scaling between single- and dual-unit reactors), a dual-unit LWR has a TCC per unit power of \$1400/kW_e and produces electricity for 3.5¢/kW_eh (2.3¢ for capital, 0.8¢ for fuel, and 0.4¢ for operation and maintenance).

On the basis of these figures, the COE for a dual-unit HYLIFE plant is 66% higher than that for a dual-unit LWR. In Fig. 18, the capital cost contribution to the COE is broken down into three components. The fuel-pellet factory contributes 0.3¢/kW_eh and the laser capital cost adds 1.1¢/kW_eh. The COE due to the HYLIFE reactor itself is 3.7¢/kW_eh, which is approximately 60% higher than the capital component of the LWR.

Table 9. Total indirect capital cost (TIC), time-related costs, and total capital cost. The dual-unit plant has a higher total capital cost but a lower cost of electricity than the single-unit plant.

	Single unit (\$ million)	Dual unit (\$ million)
Total direct cost (TDC)	2514	3895
Total indirect costs (35% of TDC)		
Construction facilities, equipment, and services	377	584
Engineering and construction management	377	584
Owner's cost	126	195
	880	1363
Time-related costs (17% of the sum of TIC and TDC)		
Interest during construction	577	894
Escalation during construction	0	0
	577	894
Total capital cost	3971	6152
Cost per unit power	\$3932/kW_e	\$3046/kW_e
Busbar cost of electricity	7.5%/kW_e	5.8¢/kW_e

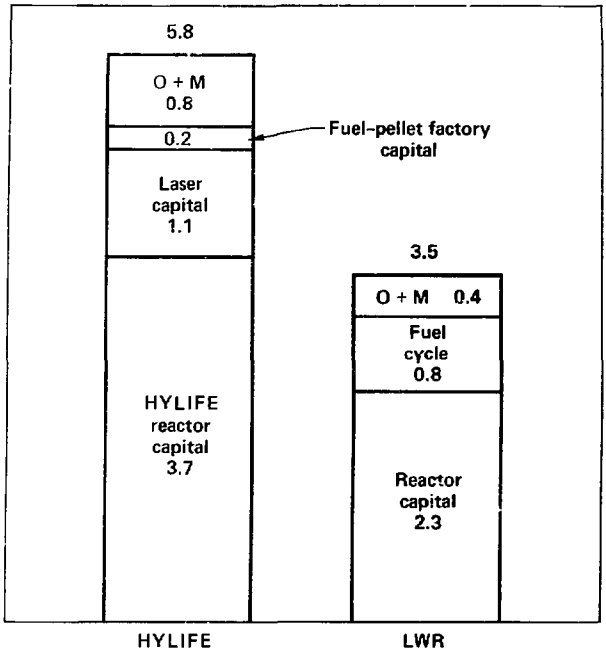

Figure 18. Comparison of the cost of electricity (¢/kW$_e$h) for HYLIFE and an LWR, both 2-GW$_e$, dual-unit plants.

The higher capital cost for the HYLIFE reactor is primarily the result of net power.[122] In fact, Bechtel's cost estimate for the HYLIFE reactor was based on LMFBR cost estimates. Some savings might be realized by doing a more careful cost analysis of the HYLIFE reactors, taking into account the inherent differences between fission and fusion reactors.

That 135 MW$_e$ are recirculated to the laser also contributes to HYLIFE's higher cost of electricity when compared to the LWR. If an additional 135 MW$_e$ were available for sale, the COE for HYLIFE would be ~5.1¢/kW$_e$h. On this basis, the capital cost of the HYLIFE reactor is $1990/kW$_e$, or 42% higher than the LWR capital cost.

7. Conclusions

We have presented a consistent conceptual design of the HYLIFE (High-Yield Lithium-Injection Fusion-Energy) concept for converting inertial confinement fusion energy into electrical power. We have examined critical issues and have found the design to be viable.

HYLIFE has many advantages. It can be built using today's technology because we chose a standard ferritic steel for the wall material and followed the methodology of the ASME Pressure Vessel Code when designing the reactor. Moreover, the reactor itself is compact, only 5 m in radius. It is also designed to last the power plant's entire 30-year lifetime without being replaced. The wall of the reactor is protected by a flowing liquid-lithium blanket that breeds tritium to replace that which is burned in the fusion reactions. The lithium also acts as a heat-transfer medium.

The tritium-breeding ratio can be adjusted below the 1.75 design value as desired. Activation of the wall material is an order of magnitude below that in comparable magnetic fusion designs.

Furthermore, the driver is separable from the reactor and power plant so that each can be developed, manufactured, and maintained as independent units. The driver can also be used for several reactors, thereby offering potential cost savings.

Even though HYLIFE's costs are higher than those for an LWR, fusion is perceived to be safer than fission, has a nearly limitless fuel supply, and mitigates the radioactive waste-disposal problem. These advantages, plus potential cost savings not considered in the HYLIFE study, make fusion a particularly viable concept for producing electrical power for future generations.

Acknowledgments

We would like to extend our appreciation to the many people and companies who contributed to the research and development of the HYLIFE concept for inertial confinement fusion (ICF). We especially thank Michael Monsler for the HYLIFE concept itself and James Maniscalco and Wayne Meier for the initial patent of the liquid-metal waterfall.

Below is a list of the major contributors to HYLIFE. We apologize if anyone was inadvertently omitted.

LLNL
Alire, R. M.
Blink, J. A.
Glenn, L. A.
Hovingh, J.
Kang, S. W.
Lasché, G. P.
Maniscalco, J. A.
Meier, W. R.
Monsler, M. J.
Pitts, J. H.
Sherohman, J. W.
Walker, P. E.
Young, D. A.

E.T.E.C., Rockwell International
Baker, R.
Darnell, A.
Hoffman, N. J.
Lamph, J. S.
McDowell, M. W.
Murray, K. A.

U.C. Davis
Asare, H. R.
Hoffman, M.
Hoover, W. G.
Monson, R. D.
Takahashi, R. K.

Energy Systems Group, Rockwell International
Goodman, M.
Kramer, D.
Martin, A. B.
Thomson, W. B.

Colorado School of Mines
Anderson, T. L.
Eberhard, B. A.
Edwards, G. R.
Wilkinson, B.

Bechtel National, Inc.
Allen, W. O.
Caird, J.
Massey, J.
Simpson, J. E.
Thomson, S.
Wood, T. J.

Grumman Aerospace Corporation
Botwin, R.
Luzzi, T.
Ojalvo, I.
Powell, E.
Sedgley, D.

References

1. M. J. Monsler et al., *Electric Power from Laser Fusion: The HYLIFE Concept*, Lawrence Livermore National Laboratory, Livermore, Calif., UCRL-812259, Rev. 1 (1978).
2. J. A. Blink and M. J. Monsler, *Status of Inertial Fusion and Prospects for Practical Power Plants*, Lawrence Livermore National Laboratory, Livermore, Calif., UCRL-89429 (1982).
3. *Laser Program Annual Report—77*, Lawrence Livermore National Laboratory, Livermore, Calif., UCRL-50021-77 (1978), pp. 8-21 to 8-25.
4. *Laser Program Annual Report—78*, Lawrence Livermore National Laboratory, Livermore, Calif., UCRL-50021-78 (1979), pp. 9-19 to 9-21.
5. *Laser Program Annual Report—78*, Lawrence Livermore National Laboratory, Livermore, Calif., UCRL-50021-78 (1979), pp. 9-33 to 9-37.
6. J. A. Blink, O. H. Krikorian, and N. J. Hoffman, "Use of Lithium in Fusion Reactors," *American Chemical Society Symposium Series*, **179**, 497–542 (1982). See also N. J. Hoffman, J. A. Blink, and A. Darnell, "Properties of Lead-Lithium Solutions," *Proc. 4th ANS Top. Meet. Technol. of Controlled Nuclear Fusion* (King of Prussia, Penn., 1980) and *1980 Laser Program Annual Report*, Lawrence Livermore National Laboratory, Livermore, California, UCRL-50021-80 (1981), pp. 9-43 to 9-47 and 9-25 to 9-26.
7. *1981 Laser Program Annual Report*, Lawrence Livermore National Laboratory, Livermore, Calif., UCRL-50021-81 (1982), pp. 8-34 to 8-36. See also J. A. Blink, "HYLIFE Design Parameters," Lawrence Livermore National Laboratory. Livermore, Calif., Internal Memo, E&MA 81-013 (Feb. 26, 1983).
8. E. F. Plechaty and J. R. Kimlinger, *TARTNP: A Coupled Neutron-Photon Monte Carlo Transport Code*, Lawrence Livermore National Laboratory, Livermore, Calif., UCRL-50400, Vol. 14 (1975).
9. E. F. Plechaty, D. E. Cullen, R. J. Howerton, and J. R. Kimlinger, *Tabular and Graphical Presentation of 175 Neutron-Group Constants Derived from the LLNL Evaluated Nuclear Data Library (ENDL)*, Lawrence Livermore National Laboratory, Livermore, Calif., UCRL-50400, Vol. 16 (1978).
10. W. R. Meier, "Two-Dimensional Neutronics Calculation for the High Yield Lithium Injection Fusion Energy Converter," *Nucl. Technol.* **52**, 22–31 (January 1981).
11. W. R. Meier, "Neutron Leakage Through Chamber Ports: A Comparison of Lithium and Lead-Lithium Blankets," *Nucl. Technol. Fusion* **3**, 385–389 (May 1983).
12. W. R. Meier, "Neutronic Implications of Lead-Lithium Blankets," *Proc. 12th Symp. Fusion Technol., Julich, FRG* (Julich, FRG, 1982). See also UCRL-87499, Lawrence Livermore National Laboratory, Livermore, Calif. (1982).
13. J. A. Blink and P. Walker, "Recent TARTNP Run," Internal Memo, SS&A 78-021, Lawrence Livermore National Laboratory, Livermore, Calif. (Feb. 1, 1978).
14. W. R. Meier, "Tritium Breeding Management in the HYLIFE Chamber," Lawrence Livermore National Laboratory, Livermore, Calif., UCRL-83969 (1980). See also *Nucl. Technol.* **52**, 170–178 (Feb. 1981).
15. W. R. Meier and W. B. Thomson, "Conceptual Design Considerations and Neutronics of Lithium Fall Laser Fusion Target Chambers," *Proc. 3rd Top. Meet. Technol. Controlled Nucl. Fusion* (Santa Fe, N. Mex., May 9–11, 1978), p. 297. See also UCRL-80782, Lawrence Livermore National Laboratory, Livermore, Calif. (1978).
16. *Laser Program Annual Report 83*, Lawrence Livermore National Laboratory, Livermore, Calif., UCRL-50021-83 (1984), pp. 7-65 to 7-68.
17. L. A. Glenn, "Divergent Impulsive Crossflow Over Packed Columnar Arrays," *Nucl. Eng. Des.* **56**, 429–437 (1980). See also *1980 Laser Program Annual Report*, Lawrence Livermore National Laboratory, Livermore, Calif., UCRL-50021-80 (1981), pp. 8-28 to 8-33.
18. L. A. Glenn, *The Influence of Radiation Transport on Lithium Fall Motion in an ICF Reactor*, Lawrence Livermore National Laboratory, Livermore, Calif., UCID-18573 (1980). See also *Laser Program Annual Report–79*, Lawrence Livermore National Laboratory, Livermore, Calif., UCRL-50021-79 (1980) pp. 8-20 to 8-28.
19. L. A. Glenn, "Transport Processes in an Inertial Confinement Fusion Reactor," *Nucl. Eng. Design* **64**, 375 (1981). See also UCRL-85061, Lawrence Livermore National Laboratory, Livermore, Calif. (1980)

and *1980 Laser Program Annual Report*, Lawrence Livermore National Laboratory, Livermore, Calif., UCRL-50021-80 (1981) pp. 9-30 to 9-42.

20. *Laser Program Annual Report 83*, Lawrence Livermore National Laboratory, Livermore, Calif., UCRL-50021-83 (1984), pp. 7-54 to 7-60.
21. J. A. Blink "Dissipation in the HYLIFE Jets," Lawrence Livermore National Laboratory, Livermore, Calif., Internal Memorandum E&MA 80-191 (October 23, 1980).
22. L. A. Glenn, "On the Motion Following Isochoric Heating of Concentric Liquid Annuli," *Nucl. Eng. Design* 60, 327 (1980). See also UCRL-84003, Lawrence Livermore National Laboratory, Livermore, Calif. (1980) and *Laser Program Annual Report—79*, Lawrence Livermore National Laboratory, Livermore, Calif., UCRL-50021-79 (1980), pp. 8-46 to 8-57.
23. L. A. Glenn, "A 2-D Model of Plasma-Jet Interaction in the HYLIFE Inertial Confinement Fusion Reactor," *Nucl. Eng. Des.* **69**(1), 75–86 (April 1982). See also *1981 Laser Program Annual Report*, Lawrence Livermore National Laboratory Livermore, Calif., UCRL-50021-81 (1982), pp. 8-36 to 8-41.
24. J. Hovingh, S. Thomson, and J. A. Blink, *Fluid Dynamics Considerations for Liquid Wall Inertially Confined Fusion Reactions*, Lawrence Livermore National Laboratory, Livermore, Calif., UCRL-82894. See also *Proc. 8th Sym. Engineering Problems of Fusion Research* (San Francisco, Calif., November, 1979) and *Laser Program Annual Report—79*, Lawrence Livermore National Laboratory, Livermore, Calif., UCRL-50021-79 (1980), pp. 8-65 to 8-68.
25. J. Hovingh and J. A. Blink, *Parametric Analysis of Stress in the ICF HYLIFE Converter Structure*, Lawrence Livermore National Laboratory, Livermore, Calif., UCRL-84272 (1980). See also *Proc. 4th Top. Meet. Technol. Controlled Nucl. Fusion* (King of Prussia, Penn., Oct 1980), USDOE Conf-801011, p. 1152.
26. L. A. Glenn and D. A. Young, "Dynamic Loading of the Structural Wall in a Lithium-Fall Fusion Reactor," *Nucl. Eng. Des.* **54**, 1 (1979). See also UCRL-82125, Lawrence Livermore National Laboratory, Livermore, Calif. (1978) and *Laser Program Annual Report—79*, Lawrence Livermore National Laboratory, Livermore, Calif., UCRL-50021-79 (1980), pp. 8-39 to 8-46.
27. J. Hovingh and J. A. Blink, "Response of Lithium Fall to Chamber Pressure," Lawrence Livermore National Laboratory, Livermore, Calif., Internal Memo SS&A 78-060 (April 12, 1978).
28. J. A. Blink, "Wall Loading of the HYLIFE Chamber," Lawrence Livermore National Laboratory, Livermore, Calif., Internal Memo SS&A 78-141 (September 1978).
29. J. Hovingh, J. A. Blink, and L. A. Glenn, "Response of a Lithium Fall to an Inertially Confined Fusion Micro Explosion," *Proc. 3rd ANS Top. Meet. Technol. of Controlled Nuclear Fusion*, DOE CONF-780508, pp. 308–317 (1978). See also *Laser Program Annual Report—77*, Lawrence Livermore National Laboratory, Livermore, Calif., UCRL-50021-77 (1978), pp. 8-37 to 8-44.
30. *1980 Laser Program Annual Report*, Lawrence Livermore, National Laboratory, Livermore, Calif., UCRL-50021-80 (1981), pp. 9-42 to 9-43.
31. *Laser Program Annual Report —77*, Lawrence Livermore National Laboratory, Livermore, Calif., UCRL-50021-77 (1978). pp. 8-36 to 8-37.
32. S. W. Kang, "Jet Stability in the Lithium Fall Reactor," *Proc. 3rd Top. Meet. Technol. of Controlled Nucl. Fusion* (Santa Fe, N. Mex., May 1980), p. 318.
33. S. W. Kang, *The Lithium Fall Reactor Concept—The Question of Jet Stability, with Recommendations for Further Experiments*, Lawrence Livermore National Laboratory, Livermore, Calif., UCRL-52531 (1978).
34. R. K. Takahashi, *Experimental Investigation of the Stability of Liquid Sheet Jets*, M.S. Thesis, University of California, Davis, Calif. (Dec. 1978).
35. M. A. Hoffman and R. K. Takahashi, *Annular Liquid Jet Experiments*, Lawrence Livermore National Laboratory, Livermore, Calif., UCRL-13938 (1980).
36. M. A. Hoffman, R. K. Takahashi, and R. D. Monson, "Annular Liquid Jet Experiments," *J. Fluids Engineering* **102**, 344–349 (September 1981).
37. R. K. Takahashi and M. A. Hoffman, *Experimental Investigation on the Stability of Liquid Sheet Jets*, Lawrence Livermore National Laboratory, Livermore, Calif., UCRL-15033 (1979).
38. *Laser Program Annual Report—78*, Lawrence Livermore National Laboratory, Livermore, Calif., UCRL-50021-78 (1979), pp. 9-14 to 9-19.

39. *Laser Program Annual Report—79*, Lawrence Livermore National Laboratory, Livermore, Calif., UCRL-50021-79 (1980), pp. 8-16 to 8-20.
40. H. R. Asare, R. K. Takahashi and M. A. Hoffman, *Liquid Sheet Jet Experiments: Comparison with Linear Theory*, Lawrence Livermore National Laboratory, Livermore, Calif., UCRL-15314 (1980). See also *J. Fluids Engineering* **103**, 595 (Dec. 1981).
41. H. R. Asare, *Theoretical and Experimental Investigation of Water Sheet Jets Under Forced Vibration*, Ph.D. Thesis, University of California, Davis, Calif. (Nov. 1980).
42. H. R. Asare and M. A. Hoffman, *Liquid Sheet Jet Experiments: Comparison with Nonlinear Theory*, Lawrence Livermore National Laboratory, Livermore, Calif., UCRL-15367 (1980).
43. *1980 Laser Program Annual Report*, Lawrence Livermore National Laboratory, Livermore, Calif., UCRL-50021-80, pp. 9-51 to 9-56 (1981).
44. R. D. Monson, *Experimental Studies of Cylindrical and Sheet Water Jets with and without Forced Nozzle Vibrations*, M.S. Thesis, University of California, Davis, Calif. (Dec. 1980).
45. M. A. Hoffman, *Liquid Jet Experiments: Relevance to Inertial Confinement Fusion Reactors*, Lawrence Livermore National Laboratory, Livermore, Calif., UCRL-15367 (1981). See also *Proc. 9th Symp. Eng. Prob. of Fusion Research* (Chicago, Ill., Oct. 1981), p. 1901.
46. *1981 Laser Program Annual Report*, Lawrence Livermore National Laboratory, Livermore, Calif., UCRL-50021-81 (1982), pp. 8-41 to 8-44.
47. J. A. Blink, *Fragmentation of Suddenly Heated Liquids*, Ph.D. Thesis, University of California, Davis, Calif. (Dec. 1984) and UCRL-53604, Lawrence Livermore National Laboratory, Livermore, Calif. (1985). See also J. A. Blink and W. G. Hoover, "Fragmentation of Suddenly Heated Liquids," *Phys. Rev. A* **32**(5), 1027 (1985), and J. A. Blink and W. G. Hoover, "Fragmentation of Suddenly Heated Liquids in ICF Reactors, *Proc. 6th ANS Top. Meet. Technol. of Fusion Energy* (San Francisco, Calif., March 1985).
48. L. A. Glenn, Lawrence Livermore National Laboratory, Livermore, Calif., private communication (August 10, 1978).
49. J. Hovingh, "First Wall Response to Energy Deposition in Conceptual Laser-Fusion Reactors," *J. Nucl. Mat.* **63**, 158 (1976).
50. J. Hovingh, *Design Considerations in Inertially Confined Fusion Reactors*, Lawrence Livermore National Laboratory, Livermore, Calif., UCRL-78499 (1976).
51. J. Hovingh, "Heat Transfer in Inertial Confinement Fusion Reactor Systems," *Nucl. Eng. Des.* **68**, 283 (1981).
52. *Laser Program Annual Report—78*, Lawrence Livermore National Laboratory, Livermore, Calif., UCRL 50021-78 (1979), pp. 9-11 to 9-14.
53. *Laser Program Annual Report—79*, Lawrence Livermore National Laboratory, Livermore, Calif., UCRL 50021-79 (1980), pp. 8-72 to 8-74.
54. *1980 Laser Program Annual Report*, Lawrence Livermore National Laboratory, Livermore, Calif., UCRL-50021-80 (1981), pp. 9-71 to 9-75.
55. R. Bullis et al., *Inertial Confinement Fusion Research and Development Studies*, Lawrence Livermore National Laboratory, Livermore, Calif., UCRL-15292 (1980), pp. 2-10 to 2-20.
56. J. H. Pitts and I. U. Ojalvo, "Design Consideration of the HYLIFE Nozzle Plate," *Res. Mechanica* **231** (1981).
57. J. H. Pitts and I. U. Ojalvo, "Fluid and Structural Dynamic Design Considerations of the HYLIFE Nozzle Plate," *Trans. 6th Intl. Conf. of Structural Mech. in Reactor Technol.* (Paris, France, 1981), paper N/53. See also UCRL-84874, Lawrence Livermore National Laboratory, Livermore, Calif. (1981).
58. J. H. Pitts, "Fatigue Crack Growth in Inertial Confinement Fusion Reaction Chamber Components," *Nucl. Technol./Fusion* **3**, 149 (1983).
59. *Laser Program Annual Report—78*, Lawrence Livermore National Laboratory, Livermore, Calif., UCRL-50021-78 (1979), pp. 9-37 to 9-43.
60. J. Hovingh and J. A. Blink, "Thermal Stress in the HYLIFE First Structural Wall," Lawrence Livermore National Laboratory, Livermore, Calif., Informal Note SS&A 78-154 (October 1978).
61. *ASME Boiler and Pressure Vessel Code*, Code Case N-47 (1980).

62. J. H. Pitts, "A Consistent HYLIFE Wall Design that Withstands Transient Loading Conditions," *Proc. 4th Top. Meet. Technol. Controlled Nucl. Fusion* (King of Prussia, Penn., July 1981), p. 1174. See also UCRL-84271, Lawrence Livermore National Laboratory, Livermore, Calif. (1981).
63. *Laser Program Annual Report—79,* Lawrence Livermore National Laboratory, Livermore, Calif., UCRL-50021-79 (1980), pp. 8-57 to 8-65.
64. *1980 Laser Program Annual Report,* Lawrence Livermore National Laboratory, Livermore, Calif., UCRL-50021-80 (1981), pp. 9-76 to 9-79.
65. J. Hovingh, *Materials Considerations for Inertially Confined Fusion Reactors (ICFR),* Lawrence Livermore National Laboratory, Livermore, Calif., UCRL-81206 (1978). See also *Proc. IEEE Minicourse on ICF* (Montreal, Canada, 1979).
66. J. A. Maniscalco, D. H. Berwald and W. R. Meier, "The Material Implication of Design and System Studies for Inertial Confinement Fusion Systems," *Fusion Reactor Materials* (North Holland Publishing Company, Amsterdam 1979), p. 37.
67. G. L. Kulcinski, "The Newest Frontier in Radiation Damage Research—Laser Fusion Reactors," *Proc. 3rd Top. Meet. Technol. Controlled Nucl. Fusion* (Santa Fe, N. Mex., May 1978), p. 598.
68. *Laser Program Annual Report—77,* Lawrence Livermore National Laboratory, Livermore, Calif., UCRL-50021-77 (1978), pp. 8-14 to 8-18.
69. Energy Systems Group, Rockwell International Corp., *Conceptual Design Study of the HYLIFE Lithium Fall Laser Fusion Chamber,* Lawrence Livermore National Laboratory, Livermore, Calif., UCRL-15219 (1979).
70. M. K. Booker, J. P. Strizak, and C. R. Brunkman, *Analysis of the Continuous Cycling Behavior of 2-1/4 Cr-1 Mo Steel,* Oak Ridge National Laboratory, Oak Ridge, Tenn., ORNL-5593 (1979).
71. *Laser Program Annual Report—79,* Lawrence Livermore National Laboratory, Livermore, Calif., UCRL-50021-79 (1980), pp. 8-95 to 8-96.
72. *Nuclear System Materials Handbook, Vol. I, Design Data,* Hanford Engineering Development Laboratory, Richland, Wash., TID-26666.
73. *Laser Program Annual Report—79,* Lawrence Livermore National Laboratory, Livermore, Calif., UCRL-50021-79 (1980), pp. 8-88 to 8-93.
74. *Laser Program Annual Report—79,* Lawrence Livermore National Laboratory, Livermore, Calif., UCRL-50021-79 (1980), pp. 8-93 to 8-95.
75. T. L. Anderson, *An Evaluation of the Corrosion Resistance of 2-1/4 Cr-1 Mo Steel in a Lithium-Lead Liquid,* M.S. Thesis, T-2372, Colorado School of Mines, Golden, Colo. (May 1980).
76. *1980 Laser Program Annual Report,* Lawrence Livermore National Laboratory, Livermore, Calif., UCRL-50021-80 (1981), pp. 9-26 to 9-30.
77. T. L. Anderson and G. R. Edwards, "The Corrosion Susceptibility of 2-1/4 Cr-1 Mo Steel in a Lithium-17.6 w/o Lead Liquid," *J. Mat. Energy Systems* **2**, 16 (1981).
78. *1981 Laser Program Annual Report,* Lawrence Livermore National Laboratory, Livermore, Calif., UCRL-50021-81 (1982), pp. 8-11 to 8-14.
79. B. D. Wilkinson, *The Corrosion Susceptibility of 2-1/4 Cr-1 Mo Steel in Lithium Lead Liquids,* M.S. Thesis, Colorado School of Mines, Golden, Colo. (1982).
80. B. D. Wilkinson, G. R. Edwards, and N. J. Hoffman, "The Effect of Lead Concentration on Corrosion Susceptibility of 2-1/4 Cr-1 Mo Steel in a Lead-Lithium Liquid," *J. Nucl. Mat.* **103-104**, 669 (1981).
81. B. Wilkinson and G. R. Edwards, *An Evaluation of 2-1/4 Cr-1 Mo Steel for Liquid Lithium Containment: III. Effect of Velocity and Lead Content,* Lawrence Livermore National Laboratory, Livermore, Calif., UCRL-15518 (1981).
82. *1982 Laser Program Annual Report,* Lawrence Livermore National Laboratory, Livermore, Calif., UCRL-50021-82 (1983), pp. 8-51 to 8-53.
83. *Laser Program Annual Report 83,* Lawrence Livermore National Laboratory, Livermore, Calif., UCRL-50021-83 (1984), pp. 7-68 to 7-73. See also B. A. Eberhard and G. R. Edwards, *The Susceptibility of 2-1/4 Cr-1 Mo Steel to Liquid-Metal-Induced Embrittlement by Lithium-Lead Solutions,* Lawrence Livermore National Laboratory, Livermore, Calif., UCRL-15639 (1984).
84. J. L. Emmett, W. F. Krupke, and J. B. Trenholme, *The Future Development of High-Power Solid State Laser Systems,* Lawrence Livermore National Laboratory, Livermore, Calif., UCRL-53344 (1982).
85. *Laser Program Annual Report—79,* Lawrence Livermore National Laboratory, Livermore, Calif., UCRL-50021-79 (1980), pp. 8-80 to 8-82.

86. *Laser Program Annual Report—79*, Lawrence Livermore National Laboratory, Livermore, Calif., UCRL-50021-79 (1980), pp. 8-79 to 8-80.
87. *Laser Program Annual Report—77*, Lawrence Livermore National Laboratory, Livermore, Calif., UCRL-50021-77 (1978), pp. 8-50 to 8-54.
88. *Laser Program Annual Report—78*, Lawrence Livermore National Laboratory, Livermore, Calif., UCRL-50021-78 (1979), pp. 9-55 to 9-67.
89. E. F. Plechaty, D. E. Cullen, and R. J. Howerton, *Tables and Graphs of Photon Interaction Cross-sections from 1.0 keV to 100 MeV Desired from the LLL Evaluated Nuclear Data Library*, Lawrence Livermore National Laboratory, Livermore, Calif., UCRL-50400, Vol. 6, Rev. 1 (1975).
90. M. J. Monsler, *Laser Fusion: An Assessment of Pellet Injection, Tracking, and Beam Pointing*, Lawrence Livermore National Laboratory, Livermore, Calif., UCRL-80563 (1978). See also *Proc. 3rd ANS Top. Meet. Nucl. Fusion* (Santa Fe, N. Mex., May 9–11, 1978), pp. 1186 to 1197.
91. J. H. Pitts, *Heat Transfer Limitations on Pellets Used in ICF Reaction Chambers*, Lawrence Livermore National Laboratory, Livermore, Calif., UCRL-85975 (1981). See also *Proc. 9th Symp. Eng. Problems of Fusion Reaseach* (Chicago, Ill., October 26–29, 1981), pp. 676 to 679.
92. *1980 Laser Program Annual Report*, Lawrence Livermore National Laboratory, Livermore, Calif., UCRL-50021-80 (1981), pp. 9-56 to 9-58.
93. V. A. Maroni, R. D. Wolson, and G. E. Strahl, "Some Preliminary Considerations of a Molten-Salt Extraction Process to Remove Tritium From Liquid Lithium Fusion Reactor Blankets," *Nucl. Technol.* 25, 83 (1975).
94. W. F. Calaway, "Electrochemical Extraction of Hydrogen From Molten LiF-LiCl-LiBr and its Application to Liquid-Lithium Fusion Reactor Blanket Processing," *Nucl. Technol.* 39, 63 (1978).
95. W. R. Meier, "Build-Up of Tritium in a Liquid Lithium Breeding Blanket for an Inertial Confinement Fusion Chamber," *Proc. 9th Symp. Eng. Problems of Fusion Research* (Chicago, Ill., October 26–29, 1981).
96. *Laser Program Annual Report—78*, Lawrence Livermore National Laboratory, Livermore, Calif, UCRL-50021-78 (1979), pp. 9-43 to 9-50.
97. *Laser Program Annual Report—78*, Lawrence Livermore National Laboratory, Livermore, Calif., UCRL-50021-78 (1979), p 9-51 to 9-55.
98. *1982 Laser Program Annual Report*, Lawrence Livermore National Laboratory, Livermore, Calif, UCRL-50021-82 (1983), pp. 8-48 to 8-51.
99. R. S. Baker, J. A. Blink, and M. J. Tessier, *Electromagnetic Pumping of Liquid Lithium in Inertial Confinement Fusion Reactors*, Lawrence Livermore National Laboratory, Livermore, Calif., UCRL-53356 (1983).
100. *Laser Program Annual Report—79*, Lawrence Livermore National Laboratory, Livermore, Calif., UCRL-50021-79 (1980), pp. 8-68 to 8-70.
101. Bechtel Group, Inc., Research and Engineering, *Conceptual Design of a Laser Fusion Power Plant, Part I, An Integrated Facility*, Lawrence Livermore National Laboratory, Livermore, Calif., UCRL-15467, Part 1 (1981).
102. *1981 Laser Program Annual Report*, Lawrence Livermore National Laboratory, Livermore, Calif., UCRL-50021-81 (1982), pp. 8-20 to 8-27.
103. *Conceptual Design Study of the HYLIFE Lithium Waterfall Laser Fusion Facility*, Bechtel National, Inc., Research and Engineering, San Francisco, Calif. (1978).
104. *1981 Laser Program Annual Report*, Lawrence Livermore National Laboratory, Livermore, Calif., UCRL-50021-81 (1982), pp. 8-31 to 8-33.
105. P. E. Walker, *Environment and Safety Features of a Lawrence Livermore Laboratory Laser Fusion Reactor Design*, Lawrence Livermore National Laboratory, Livermore, Calif., UCRL-80564 (1978).
106. P. E. Walker, *Remote Systems Requirements of the HYLIFE Converter Concept*, Lawrence Livermore National Laboratory, Livermore, Calif., UCRL-81309 (1978).
107. *Laser Program Annual Report—77*, Lawrence Livermore National Laboratory, Livermore, Calif., UCRL-50021-77 (1978), pp. 8-93 to 8-95.
108. *Laser Program Annual Report—78*, Lawrence Livermore National Laboratory, Livermore, Calif., UCRL-50021-78 (1979), pp. 9-67 to 9-75.

109. J. A. Blink, R. E. Dye, and J. R. Kimlinger, *ORLIB: A Computer Code that Produces One-Energy Group, Time- and Spatially Averaged Neutron Cross Sections*, Lawrence Livermore National Laboratory, Livermore, Calif., UCRL-53262 (1981).
110. J. A. Blink, *FORIG: A Modification of the ORIGEN2 Isotope-Generation and Depletion Code for Fusion Problems*, Lawrence Livermore National Laboratory, Livermore, Calif., UCRL-53263 (1982).
111. *1981 Laser Program Annual Report*, Lawrence Livermore National Laboratory, Livermore, Calif., UCRL-50021-81 (1982), pp. 8-28 to 8-30.
112. G. P. Lasché and J. A. Blink, *The Dependence of Neutron Induced Radioactivity in Fusion Reactors on Geometric Design Parameters*, Lawrence Livermore National Laboratory, Livermore, Calif., UCRL-88212 (1983).
113. J. A. Blink and G. P. Lasché, *Influence of Steel Type on the Activation and Decay of Fusion Reactor First Walls*, Lawrence Livermore National Laboratory, Livermore, Calif., UCRL-88211 (1983).
114. J. A. Blink, *Neutron Activation of Four Ferritic Steels*, Lawrence Livermore National Laboratory, Livermore, Calif., UCID-19823 (1983).
115. *Laser Program Annual Report 83*, Lawrence Livermore National Laboratory, Livermore, Calif., UCRL-50021-83 (1984), pp. 7-76 to 7-80.
116. *1981 Laser Program Annual Report*, Lawrence Livermore National Laboratory, Livermore, Calif., UCRL-50021-81 (1982), pp. 8-44 to 8-46.
117. *1983 Laser Program Annual Report*, Lawrence Livermore National Laboratory, Livermore, Calif., UCRL-50021-83 (1984), pp. 7-73 to 7-76.
118. J. A. Blink, D. W. Dorn, and R. C. Maninger, "Disposal of Activated Fusion Materials," *Proc. 3rd Top. Meet. Fusion Reactor Materials* (Albuquerque, N. Mex., September 19-22, 1983).
119. *1980 Laser Program Annual Report*, Lawrence Livermore National Laboratory, Livermore, Calif., UCRL-50021-80 (1981), pp. 9-25 to 9-26.
120. *1980 Laser Program Annual Report*, Lawrence Livermore National Laboratory, Livermore, Calif., UCRL-50021-80 (1981), pp. 9-79 to 9-88.
121. *Energy Economic Data Base Program—Phase VI Update Report*, United Engineers and Constructors Report, UE&C-ANL-840630 (1983).
122. Bechtel Engineering Group, *Conceptual Design of a Laser Fusion Power Plant*, Lawrence Livermore National Laboratory, Livermore, Calif., UCRL-15467, part 1 (1981), p. 35.
123. *Laser Program Annual Report—79*, Lawrence Livermore National Laboratory, Livermore, Calif., UCRL-50021-79 (1980), pp. 8-119 to 8-127.
124. K. A. Bruekner, *Assessment of Drivers and Reactors for Inertial Confinement Fusion*, EPRI Report AP-1371 (1980).
125. J. W. Sherohman and W. R. Meier, "A Parametric Study of a Target Factory for Laser Fusion," *Proc. 4th Top. Meet. Technol. of Controlled Nucl. Fusion* (King of Prussia, Penn., October 14-17, 1980), p. 1182.
126. D. H. Berwald and W. R. Meier, "Reactor Systems Modelling for ICF Hybrids," *Proc. 4th Top. Meet. Technol. of Controlled Nucl. Fusion* (King of Prussia, Penn., October 14-17, 1980), p. 1487.
127. S. C. Schulte, T. L. Willke, and J. R. Young, *Fusion Reactor Design Studies—Standard Accounts for Cost Estimates*, Pacific Northwest Laboratory Report, PNL-2648 (1978).

KLE/lb

Appendix A. Annotated Bibliography

Laser Program Annual Reports Applicable to HYLIFE

The *Laser Program Annual Reports* (*LPARs*) document the results of laser research at Lawrence Livermore National Laboratory, Livermore, Calif. Specifically, advancements in the HYLIFE reactor study are documented in the Energy and Military Applications section of the *1978* through *1984 LPARs*. Studies applicable to the HYLIFE reactor were also documented in the *1977 LPAR*. Listed below are those articles concerned with HYLIFE. The titles are taken from the table of contents of the 1977 through the 1984 *LPARs*.

Laser Program Annual Report—77, Lawrence Livermore National Laboratory, Livermore, Calif., UCRL-50021-77 (1978), pp. 8-1 to 8-95.

Overview
Conceptual Design Study
- Performance Parameters
- Reactor, Optical, and Laser Systems
- Liquid-Metal Circulation System
- Liquid-Lithium Corrosion
- Cost Considerations
- Summary

Neutronic Studies for Fluid Reactors
- Energy Deposition, Tritium Breeding, and Radiation Damage
- Target-Dependent Effects

First-Wall Response and Fluid-Response Studies
- Interaction of Debris with First Wall
- Liquid Sheets and Jets
  - Jet Stability—Lithium Fall Reactors
  - Lithium Fall Response—ICF Microexplosion
  - Qualitative Response of the Fall
  - Fall Response to Neutron Energy Deposition
  - Fall Response to X Rays
  - Vaporization Effects
  - Wall Response to Liquid Impact
  - Quantitative Results
  - Discussion of Result
  - Ion-Beam Fusion Reactor Studies

Optical Design Considerations for Laser Fusion Power Plants
- Final Focusing System
- Propagation in the Target Chamber

Environmental and Safety Features

Laser Program Annual Report—78, Lawrence Livermore National Laboratory, Livermore, Calif., UCRL-50021-78 (1979), pp. 9-1 to 9-75.

Introduction
Conceptual Design of a Laser Fusion Power Plant
- Introduction
  - Our Energy Options
  - The HYLIFE Design Approach
  - The HYLIFE Design Concept
- Lithium Blanket Configuration
- Blanket Response

Materials Considerations
Chamber Design
Liquid-Metal Circulation System
Steam and Electricity Generation
Optical and Pellet-Injection Systems
Environmental and Safety Considerations

Laser Program Annual Report—79, Lawrence Livermore National Laboratory, Livermore, Calif., UCRL-50021-79 (1980), pp. 8-1 to 8-119.
Introduction
A Conceptual Design Strategy for Liquid-Metal-Wall Inertial Fusion Reactors
Introduction
Positive and Negative Features of LMW Chambers
Review of LMW Chambers
Guidelines for the Design of an LMW Chamber
New of Revised Calculations of the High-Yield Lithium-Injection Fusion-Energy (HYLIFE) System
Vibrational Analysis of the HYLIFE Chamber
Experimental Investigation of the Stability of Liquid-Sheet Jets
Central Region Pressurization Caused By X-Ray and Debris-Generated Lithium Blowoff
Outward Drag on the Jet Array by the Expanding Lithium
Neutron-Induced Specific Energy Deposition at the Chamber Midplane
Annular-Fall Response to a 750-MJ Fusion Pulse
Dissipation of Kinetic Energy by the HYLIFE Jet Array
Design Method for the HYLIFE Reaction Chamber
First-Wall Design Using Several Procedures and LMW Geometries
Removal of Noncondensible Gases from the HYLIFE Chamber—Initial Conditions
Evolution of the HYLIFE Fusion-to-Electricity Converter
Overview
HYLIFE Component Design
Nozzle Plate
Vacuum Vessel, First Structural Wall, and Reflector
Lithium Circulation
Materials Considerations
Summary
Alternative HYLIFE Design Options
Steam Cycle Options
Energy Balance for Heavy-Ion-Beam Driven HYLIFE Converter Systems
A Comparison of Mechanical and Electromagnetic Pumps
Nb-1% Zr as a First-Structural-Wall Material in the HYLIFE Converter Concept
Material Considerations for Liquid-Wall ICF Energy Converters
Structural Material Selection and Qualification in a Liquid-Metal Environment
Liquid-Lithium Corrosion of 2-1/4 Cr-1 Mo Steel Weldments
High-Cycle Fatigue Strength of 2-1/4 Cr-1 Mo Ferritic Steel at Elevated Temperatures
Analytic Lithium Equation of State
Properties of Lead-Lithium Solutions
Properties of Graphite
Cost-Performance Studies of an Inertial-Fusion Power Plant

1980 Laser Program Annual Report, Lawrence Livermore National Laboratory, Livermore, Calif., UCRL-50021-80 (1981), pp. 9-1 to 9-90.
Introduction
Accomplishments Associated with the HYLIFE Chamber Concept
Operating Parameters of Inertial Fusion
Parametric Studies

The Influence of Chamber Pulse Rate on Structural Stress and Lithium Flow
Blanket-Shield Design Options
The Effect of Chamber Ports on Neutron Leakage and Blanket Performance
Materials Considerations
Solubility of Hydrogen Isotopes in Lead-Lithium Solutions
Corrosion of 2-1/4 Cr-1 Mo in Lithium and Lead-Lithium Solutions
Fluid and Pumping Considerations
Transport Processes in the HYLIFE Reaction Chamber
Vortex-Flow Slanted-Jet Improvement to HYLIFE
Heavy-Ion-Beam Ballistic Propagation in Liquid-Metal-Wall Reaction Chambers
Experimental Plan to Measure Effects of Gas Blowing Through Jets
Experimental Investigation of the Stability with Liquid-Sheet Jets: A Comparison with Linear and Nonlinear Theory
Vacuum Pumping
Electromagnetic Pump Considerations
Lithium Safety Considerations
Build-up of Tritium in a Liquid Lithium Breeding Blanket
Component Design
Stress Analysis of the Alternate Helical Bar First Structural Wall (FSW)
Nozzle Plate
Fatigue Crack Growth in HYLIFE Components
Allowable Driver and Target Factory Cost
Engineering Test Facility (ETF) Planning

1981 Laser Program Annual Report, Lawrence Livermore National Laboratory, Livermore, Calif., UCRL-50021-81 (1982), pp. 8-33 to 8-46.
Reactor Design Studies
HYLIFE Design Progress
HYLIFE Chamber Phenomena
Jet Stability Experiments
Radioactivity in the HYLIFE Reactor

1982 Laser Program Annual Report, Lawrence Livermore National Laboratory, Livermore, Calif., UCRL-50021-82 (1983), pp. 8-34 to 8-58.
Neutron-Activation Studies
Influence of Steel Type on Fusion Wall Activation
Influence of Fusion Reactor Configuration on Neutron-Induced Radioactivity
Liquid-Metal Systems
Temperature and Velocity Limits for Liquid-Lithium Solutions
Liquid-Jet Impact Experiments
Passage of Lithium through Stainless Steel Mesh
Electromagnetic Pumping of Liquid Lithium
Embrittlement of 2-1/4 Cr-1 Mo Steel by a 1 at.% Pb-99 at.% Li Liquid
Power-Plant Considerations
Evaluation of Direct-Illumination-Driven ICF Reactors
Commercialization of Inertial Fusion for Electric Power Production

Laser Program Annual Report 83, Lawrence Livermore National Laboratory, Livermore, Calif., UCRL-50021-83 (1984), pp. 7-46 to 7-80.
General Studies and Reactor Development Technologies
Cost Goals for ICF Reactors
Development Facilities for ICF Reactor Commercialization
Disassembly of Isochorically Heated Liquids
Blanket Optimization Techniques

Dependence of Displacement Damage on Blanket Design
Susceptibility of 2-1/4 Cr-1 Mo Steel to Liquid-Metal Embrittlement
Waste Disposal
Steel Type and Impurity Effects on Activation

1984 Laser Program Annual Report, Lawrence Livermore National Laboratory, Livermore, Calif., UCRL-50021-84 (1985), pp. 7-47 to 7-64.
General Studies
Identifiying Heavy-Ion-Beam Fusion Design and System Features with High Economic Leverage
Blanket Optimization for the HYLIFE Reactor
Fragmentation of Suddenly Heated Liquids in ICF Reactors

Key HYLIFE Publications

Baker, R. S., J. A. Blink, and M. J. Tessier, *Electromagnetic Pumping of Liquid Lithium in Inertial Confinement Fusion Reactors*, Lawrence Livermore National Laboratory, Livermore, Calif., UCRL-53356 (1983).
Discusses the basic operating principles and geometries of ten electromagnetic pumps. The annular-linear-induction pump and the helical-rotor electromagnetic pump are compared for possible use in a full-scale liquid-lithium inertial confinement fusion reactor.

Bangerter, R. O. et al., *The Lawrence Livermore Laboratory Heavy Ion Fusion Program*, Lawrence Livermore National Laboratory, Livermore, Calif., UCRL-82120 (1978). See also *Proc. of the Heavy Ion Fusion Workshop* (Argonne National Laboratory, Argonne, Ill., Sept. 19–26, 1978).
Discusses the fusion program at LLNL. Included are target design, HYLIFE energy conversion chamber design, and ion beam propagation in the combustion chamber.

Bechtel Group, Inc., Research and Engineering, *Conceptual Design of a Laser Fusion Power Plant*, Lawrence Livermore National Laboratory, Livermore, Calif., UCRL-15467 (1981).
A preliminary conceptual design and economic analysis of the HYLIFE balance of plant.

Blink, J. A. and W. G. Hoover, *Disassembly of Isochorically Heated Liquids*, Lawrence Livermore National Laboratory, Livermore, Calif., UCRL-53604 (1985). See also *Proc. 3rd Intl. Conf. on Liquid Metal Eng. and Technol. in Energy Prod.* (Oxford, England, April 9–13, 1984); "Fragmentation of Suddenly Heated Liquids," *Phys. Rev. A* 32(5), 1027 (1985), and "Liquid Fragmentation in ICF Reactors,"[11] *Proc. of the 6th ANS Topical Mtg. on Technol. of Fusion Energy* (San Francisco, Calif., March 1985).
Examines thermodynamic and hydrodynamic approaches to drop-fragment-size estimation. Describes a molecular dynamics approach to verifying the hydrodynamic model. HYLIFE is used as a model.

Blink, J. A., O. H. Krikorian, and N. J. Hoffman, *The Use of Lithium in Fusion Reactors*, Lawrence Livermore National Laboratory, Livermore, Calif., UCRL-85145 (1981). See also *Proc. Am. Chem. Soc.* (Atlanta, Georgia, March 29 to April 3, 1981).
Discusses three fusion reactor concepts (including HYLIFE), engineering details for safe handling of molten lithium, and tritium recovery from the various breeding materials. Emphasis is on material selection and material compatibility with lithium.

Blink, J. A. and G. P. Lasché, *The Influence of Steel Type on the Activation and Decay of Fusion Reactor First Walls*, Lawrence Livermore National Laboratory, Livermore, Calif., UCRL-88211 (1983). See also *Proc. ANS 5th Topical Mtg. on the Technol. of Fusion Energy* (Knoxville, Tenn., April 26–28, 1983).
Compares five steels from the viewpoints of activation, afterheat, inhalation-biological-hazard potential (bhp), ingestion bhp, and feasibility of disposal by shallow land burial.

Blink, J. A. and J. A. Maniscalco, *An Engineering Development Plan For Inertial Confinement Fusion*, Lawrence Livermore National Laboratory, Livermore, Calif., UCRL-84467 (1980). See also *Proc. 15th Intersociety Energy Conservation Conf.* (Seattle, Wash., Aug. 17–22, 1980).

Describes the preliminary analysis of engineering development required for a liquid-metal wall engineering test facility. All current driver and reactor options are considered.

Blink, J. A. and M. J. Monsler, *Status of Inertial Fusion and Prospectus for Practical Power Plants*, Lawrence Livermore National Laboratory, Livermore, Calif., UCRL-89429 (1982). See also *Proc. 3rd Intern. Conf. on Emerging Nucl. Energy Systems* (Helsinki, Finland, June 6–9, 1983) and *Atomkernenergie-Kerntechnik* **43**, 205–208 (1983).

Discusses four reactor designs—HYLIFE, Pulse*Star, Cascade, and Sunburst—that meet the variety of target-driver combinations. The goals of these designs are low cost, low probability of public risk, and minimal environmental impact.

Blink, J. A. et al., *An ICF ETF and its Engineering Development Requirements*, Lawrence Livermore National Laboratory, Livermore, Calif., UCRL-84275 (1980). See also *Proc. 4th ANS Top. Mtg. on the Technol. of Controlled Nucl. Fusion* (King of Prussia, Penn., Oct. 14–17, 1980).

Outlines the current state of planning for an ICF Engineering Test Facility (ETF) and the engineering and development that must precede it.

Bullis, R. et al., *Inertial Confinement Fusion Research and Development Studies*, Lawrence Livermore National Laboratory, Livermore, Calif., UCRL-15292 (1980).

ICF research and development studies for selected structural, thermal, and vacuum pumping analyses in support of the HYLIFE concept.

Frank, T. G. et al., *Power Plant Design For Inertial Confinement Fusion—Implications for Pellets*, Lawrence Livermore National Laboratory, Livermore, Calif., UCRL-86536 (1981). See also *Proc. 28th Natl. Vacuum Symp.* (Anaheim, Calif., Nov. 3–6, 1981) and *J. Vac. Sci. Technol.* **20**(4), 1381–1387 (April 1982).

Discusses pellet concepts, reactor/driver concepts, and cavity environment for inertial confinement fusion reactors.

Glenn, L. A., *Divergent Impulsive Crossflow Over Packed Columnar Arrays*, Lawrence Livermore National Laboratory, Livermore, Calif., UCRL-83051 (1979). See also *Intern. J. of Nucl. Eng. Des.* **56**, 429–432 (Feb. 1980).

An application of a quasi one-dimensional method for calculating transient, compressible, viscous flows through packed beds and over tube bundles. The method was used to study the impulsive crossflow of a lithium plasma through an array of liquid jets.

Glenn, L. A., *On the Motion Following Isochoric Heating of Concentric Liquid Annuli*, Lawrence Livermore National Laboratory, Livermore, Calif., UCRL-84003 (1980). See also *Intern. J. of Nucl. Eng. Des.* **60**, 327-337 (Oct. 1983).

A study of the reduction in neutron-induced momentum caused by segmenting a single annulus into nested annuli separated by gaps.

Glenn, L. A., *The Influence of Radiation Transport on Lithium Fall Motion in an ICF Reactor*, Lawrence Livermore National Laboratory, Livermore, Calif., UCID-18573 (1980).

Discusses the implosion, stagnation, and radiation from and reexpansion of the lithium that is ablated from the HYLIFE jets by the fusion x rays.

Glenn, L. A., *Dynamic Loading of the Structural Wall in a Lithium Fall Fusion Reactor*, Lawrence Livermore National Laboratory, Livermore, Calif., UCRL-82125 (1978). See also *Intern. J. Nucl. Eng. Design* **54**, 1–16 (1979).

Describes events subsequent to energy deposition in the lithium annulus and how the annulus impacts the structural wall.

Glenn, L. A., *A 2-D Model of Plasma-Jet Interaction in the HYLIFE Inertial Confinement Fusion Reactor* Lawrence Livermore National Laboratory, Livermore, Calif., UCRL-86646 (1982). See also *Nucl. Eng. Design* 69, 75–86 (April 1982).

Discusses a two-dimensional, axisymmetric model developed to study the impulsive crossflow of a lithium gas through a closely packed, annular liquid-jet arrangement. Calculations performed with this model indicate that a 5-m-radius reactor cavity, standing 8 m high, can deliver 1 GWe when pulsed at 1 Hz, without adverse loading of the first wall.

Glenn, L. A., *Transport Processes in an Inertial Confinement Fusion Reactor,* Lawrence Livermore National Laboratory, Livermore, Calif., UCRL-85061 (1981). See also *Nucl. Eng. Des.* **64** (3), 375–387 (April 1981).

The quasi one-dimensional method previously developed for calculating a transient, compressible, viscous flow through a complex array of tubes or jets was extended to include heat and mass exchange between the fluid and the jets.

Glenn, L. A., *On the Fragmentation of Condensed Material By Isochoric Heating and Release,* Lawrence Livermore National Laboratory, Livermore, Calif., UCID-19737 (1983).

Extends an energy minimization model used to estimate fragment sizes from rapidly heated liquids or solids. The model is based on the concept that surface area created in the fragmentation process is governed by an equilibrium balance of the surface energy and a local (nontranslational) kinetic energy in the fragments.

Glenn, L. A. and D. A. Young, *Dynamic Loading of the Structural Wall in a Lithium Fall Fusion Reactor,* Lawrence Livermore National Laboratory, Livermore, Calif., UCRL-82125 (1978).

This article identifies two potential mechanisms for structural wall damage: surface erosion and hoop failure. It also discusses the feasibility of different lithium fall.

Hoffman, M. A. et al., *Research on the HYLIFE Liquid-First-Wall Concept for Future Laser-Fusion Reactors. Final Report No. 4,* Lawrence Livermore National Laboratory, Livermore, Calif., UCRL-15033 (1979).

Reports experimental results on planar sheet water jets subjected to forced harmonic excitation.

Hoffman, M. A., R. H. Asare, and R. D. Monson, *Research on the HYLIFE Liquid-First-Wall Concept for Future Laser-Fusion Reactors: Liquid Sheet Jet Experiments: Comparison with a Nonlinear Theory,* Lawrence Livermore National Laboratory, Livermore, Calif., UCRL-15367 (1980).

Reports experimental results on planar sheet water jets flowing vertically downward.

Hoffman, M. A. et al., *Research on the HYLIFE Liquid-First-Wall Concept for Future Laser-Fusion Reactors: Liquid Jet Experiments: Relevance to Inertial Confinement Fusion Reactors,* University of California Department of Mechanical Engineering, Davis, Calif., Final Report No. 7. (Oct. 1981).

Studies of a self-healing, renewable liquid-wall reactor.

Hoffman, M. A. and A. R. Raffray, *Research on the HYLIFE Liquid-First-Wall Concept for Future Laser-Fusion Reactors: Liquid Jet Impact Experiments,* Lawrence Livermore National Laboratory, Livermore, Calif., UCRL-15367 (1982).

Evaluation of transient- and steady-state drag on a single bar and on some selected arrays of bars by impacting liquids. Determines the momentum removed from impacting liquid slugs. An array of bars is an alternative FSW geometry, compared to the baseline solid wall.

Hoffman, M. A., R. H. Asare, and R. D. Monson, *Research on the HYLIFE Liquid-First-Wall Concept for Future Laser-Fusion Reactors: Liquid Sheet Jet Experiments: Comparison with Linear Theory,* Lawrence Livermore National Laboratory, Livermore, Calif., UCRL-15314 (1980).

Reports on experimental results for planar sheet water jets subjected to transverse forced harmonic excitation.

Hoffman, N. J. and M. W. McDowell, *Liquid Metal Engineering Aspects of a Commercial-Sized Power Plant Based on the HYLIFE Converter Concept*, Lawrence Livermore National Laboratory, Livermore, Calif., UCRL-15105 (1979).

Describes the ICF power-plant energy balance, the protective lithium-fall circuit, and the heat transfer system. Also discusses compatibility of structural alloys with lithium, and tritium separation.

Hoffman, N. J., J. Hovingh, and W. R. Meier, *Material Aspects of the HYLIFE Converter and ICF Power Plants*, Lawrence Livermore National Laboratory, Livermore, Calif., UCRL-81459, Abstract (1978).

Discusses the material considerations for the HYLIFE chamber. Some considerations are unique to HYLIFE, while others are generic to ICF systems.

Hoffman, N. J., A. Darnell, and J. A. Blink, *Properties of Lead-Lithium Solutions*, Lawrence Livermore National Laboratory, Livermore, Calif., UCRL-84273 (1980). See also *Proc. 4th ANS Top. Mtg. on the Technol. of Controlled Nucl. Fusion* (King of Prussia, Penn., Oct. 14–17, 1980).

Reviews the properties of lead-lithium solutions, the effects of hydrogen impurities, and the subsequent reactor design implications.

Hovingh, J., *Material Considerations for Inertially Confined Fusion Reactors (ICFR)*, Lawrence Livermore National Laboratory, Livermore, Calif., UCRL-81206 (1978).

Compares the material considerations for inertially confined reactors with those of magnetically confined reactors. The lithium fall reactor is used as an example of the freedom from constraints intrinsic to inertially confined fusion reactors.

Hovingh, J., *Design Issues and Material Problems in Inertially Confined Fusion Reactors*, Lawrence Livermore National Laboratory, Livermore, Calif., UCRL-82943 (1979). See also *Proc. of the Impact Fusion Workshop* (Los Alamos, N. Mex., July 10–13, 1979).

Discusses the effects of the deposition of pulsed fusion energy, the effects of the cavity environment on the fusion spectra and consequent implications on the FSW design, and the applications of these effects to the HYLIFE reactor concept.

Hovingh, J., *Heat Transfer in Inertial Confinement Fusion Reactor Systems*, Lawrence Livermore National Laboratory, Livermore, Calif., UCRL-81673 (April 23, 1980). See also *Proc. 19th Natl. Heat Transfer Conf.* (Orlando, Fla., July 27–30, 1980).

An overview of the various ICF reactor designs that attempt to reduce peak power intensities and a discussion of the heat transfer considerations for each design.

Hovingh, J., *Design Considerations for Direct-Illumination-Driven Inertial Fusion Reactors*, Lawrence Livermore National Laboratory, Livermore, Calif., UCRL-88215 (1983). See also *Proc. ANS 5th Top. Mtg. on the Technol. of Fusion Energy* (Knoxville, Tenn., April 26–28, 1983).

Parametrically examines the implications on inertial fusion reactor design of using direct drive pellets instead of radiation-driven targets. The examination includes impact of direct illumination on mirror damage constraints, reactor neutronic performance, and system energetics and cost.

Hovingh, J., J. A. Blink, and L. A. Glenn, *Response of the Laser Fusion HYLIFE Reactor Chamber to the Fusion Microexplosion*, Lawrence Livermore National Laboratory, Livermore, Calif., UCRL-81310, Summary (1978).

Expands the previous models used to analyze the response of a single annular liquid lithium fall to the 2700-MJ fusion pulse and to estimate the subsequent wall loading.

Hovingh, J., J. A. Blink, and L. A. Glenn, *Response of a Lithium Fall to an Inertially Confined Fusion Microexplosion*, Lawrence Livermore National Laboratory, Livermore, Calif., UCRL-80562 (1978). See also *Proc. 3rd Top. Mtg. on Fusion* (Santa Fe, N. Mex., May 9–11, 1978).

Discusses the response of the lithium blanket to the microexplosion products, and estimates the resulting loading and stresses in the first structural wall.

Hovingh, J. et al., *Inertial Fusion: An Energy Production Option for the Future*, Lawrence Livermore National Laboratory, Livermore, Calif., UCRL-87671 (1982). See also *Proc. 17th Intersociety Energy Conversion Eng. Conf.* (Los Angeles, Calif., Aug. 8–13, 1982).

Discusses the inertial confinement approach to fusion energy and describes fusion fundamentals, state of the art of fusion experiments, and the results achieved through the use of Nd:glass lasers.

Hovingh, J. and J. A. Blink, *Parametric Analysis of Stress in the ICF HYLIFE Converter Structure*, Lawrence Livermore National Laboratory, Livermore, Calif., UCRL-84272 (1980). See also *Proc. 4th Top. Mtg Technol. Controlled Nucl. Fusion* (King of Prussia, Penn., Oct. 1980), ANS Pub. No. CONF-801011 (1981), pp. 1152–1161.

Discusses a methodology to determine the optimum combination of liquid-metal first wall geometry and first structural wall thickness. A parametric analysis based on the methodology is presented of the liquid-metal flow rate and first structural wall requirements.

Hovingh, J., S. Thomson, and J. A. Blink, *Fluid Mechanics Considerations for Liquid Wall Inertially Confined Fusion Reactors*, Lawrence Livermore National Laboratory, Livermore, Calif., UCRL-82894, Abstract (1979). See also *Proc. 8th Symp. on Engineering Problems of Laser Research* (San Francisco, Calif., Nov. 16, 1979).

Discusses the liquid curtain concept for inertially confined fusion reactions. The primary fluid mechanics issues are the impact load of the liquid on the structure and the liquid fragmentation caused by the volumetric deposition of very intense energy fluxes.

Kang, S. W., *The Lithium Fall Reactor Concept—The Question of Jet Stability, With Recommendations for Further Experiments*, Lawrence Livermore National Laboratory, Livermore, Calif., UCRL-52531 (1978).

Analyzes and discusses jet stability with respect to fluid dynamics, delineates physical factors that may affect the jet breakup, and performs some simple calculations to determine quantitatively the relative influences of various parameters.

Kang, S. W., *Viscous Effects on a Turbulent Jet Near Nozzle Exit*, Lawrence Livermore National Laboratory, Livermore, Calif., UCRL-81826 (1979). See also *Proc. Annual Mtg. Am. Phys. Soc.* (New York, N.Y., Jan. 29 to Feb. 1, 1979).

Analysis of the viscous effects on changes in the velocity profile of an incompressible turbulent jet exhausting into an immiscible ambient medium.

Maniscalco, J. A., W. R. Meier, and M. J. Monsler, *Conceptual Design of a Laser Fusion Power Plant*, Lawrence Livermore National Laboratory, Livermore, Calif., UCRL-79652 (1977). See also *Proc. Am. Instit. Chem. Engineers* (New York, N.Y., Nov. 13–17, 1977).

Presents the preliminary results of a laser fusion power plant conceptual design that uses a thick, falling region of liquid metal.

Maniscalco, J. A., W. R. Meier, and M. J. Monsler, *Design Studies of a Laser Fusion Power Plant*, Lawrence Livermore National Laboratory, Livermore, Calif., UCRL-80081 (1977). See also *Proc. Technol. Committee and Workshop on Fusion Reactor Design* (University of Wisconsin, Madison, Wisc., Oct. 10–21, 1977).

Discusses a conceptual design of a laser fusion power plant. The design would be able to exploit new, high-gain targets in order to relax the laser and optical requirements.

Maniscalco, J. A. et al., *Civilian Applications of Laser Fusion*, Lawrence Livermore National Laboratory, Livermore, Calif., UCRL-52349 (1977).

Discusses the prospects of producing commercial electricity with laser fusion, a detailed description of the lithium waterfall reactor, and a discussion of other potential applications of laser fusion.

Maniscalco, J. A., W. R. Meier, and M. J. Monsler, *Conceptual Design of a Laser Fusion Power Plant*, Lawrence Livermore National Laboratory, Livermore, Calif., UCRL-79652 (1977).

A conceptual design study to view recent developments in advanced targets that greatly enhance the prospects for commercial laser fusion power.

Maniscalco, J. A., D. H. Berwald, and W. R. Meier, *The Material Implications of Design and System Studies for Inertial Confinement Fusions Systems*, Lawrence Livermore National Laboratory, Livermore, Calif., UCRL-82041 (1979). See also *Proc. 1st Top. Mtg. on Fusion Reactor Mat.* (Miami Beach, Fla., Jan. 29–31, 1979).

Defines and analyzes the material requirements for inertial confinement fusion reactors, and discusses the problems associated with the flow and containment of liquid lithium.

Maniscalco, J. A. and W. R. Meier, *A Comparative Study of Exploratory Reactor Concepts for Inertial Confinement Fusion*, Lawrence Livermore National Laboratory, Livermore, Calif., UCRL-79065, Summary (1977).

Discusses different reactor concepts for producing electricity with inertial confinement fusion. Issues discussed include source abundancy, safety, environmental acceptability, technical feasibility, and economic competitiveness.

Maniscalco, J. A., *Liquid Lithium Waterfall Inertial Confinement Fusion Reactor Concept*, Lawrence Livermore National Laboratory, Livermore, Calif., UCRL-79064, Summary (1977).

Discusses the study of the liquid lithium waterfall concept for inertial confinement fusion.

Meier, W. R., *Neutronic Aspects of the Lithium Fall Reactor*, Lawrence Livermore National Laboratory, Livermore, Calif., UCRL-80561, Summary (1973).

Presents a one-dimensional, spherical geometry model to determine the spatial energy deposition profile, tritium-breeding ratio, and gas-production and atomic-displacement rates in the first structural wall.

Meier, W. R., *Control Of Tritium Breeding in the Fluid Wall ICF Reactor Concept*, Lawrence Livermore National Laboratory, Livermore, Calif., UCRL-81297, Summary (1978).

Discusses several means of controlling the tritium-breeding ratio in the lithium wall: using a graphite reflector with a neutron poison, limiting the thickness of the wall to 60 cm, introducing ~3 atm.% B^{10} into the lithium stream, and denaturing lithium to about 0.5 atm.% in ^6Li.

Meier, W. R., *Neutronic Implications of Lead-Lithium Blankets*, Lawrence Livermore National Laboratory, Livermore, Calif., UCRL-87499 (1982). See also *Proc. 12th Symp. on Fusion Technol.* (Jülich, FRG, Sept. 13–17, 1982.)

Describes the neutronic characteristics of lead-lithium blankets with emphasis on the enhanced neutron leakage through chamber ports and the degradation in blanket performance parameters that occurs as a result of the enhanced leakage.

Meier, W. R., *Build-Up of Tritium in a Liquid Lithium Breeding Blanket for an Inertial Confinement Fusion Chamber*, Lawrence Livermore National Laboratory, Livermore, Calif., UCRL-85245 (1981). See also *Proc. 9th Symp. on Eng. Problems of Fusion Research* (Chicago, Ill., Oct. 26–29, 1981).

Examines the buildup of tritium in a liquid-lithium breeding blanket for an ICF reactor. Tritium break-even time and break-even inventory are defined and related to the various tritium flow rates.

Meier, W. R., *Two-Dimensional Neutronics Calculation for the HYLIFE Converter*, Lawrence Livermore National Laboratory, Livermore, Calif., UCRL-83595 (1980). See also *Nucl. Technol.* **52**, 22–31 (Jan. 1981).

Analyzes the nuclear heating and tritium-breeding characteristics of the HYLIFE converter using the coupled neutron-photon Monte Carlo transport code (TARTNP) and the LLNL Evaluated Nuclear Data Library (ENDL).

Meier, W. R., *Neutron Leakage Through Fusion Chamber Ports: A Comparison of Lithium and Lead-Lithium Blankets*, Lawrence Livermore National Laboratory, Livermore, Calif., UCRL-87331 (1982). See also *Nucl. Technol./Fusion* **3**, 385–391 (May 1983).

Discusses the Monte Carlo neutronics calculations used to compare the effects of chamber ports on the neutron leakage and blanket performance for lithium and lead-lithium blankets. TARTNP, a coupled neutron-photon Monte Carlo code, and ENDL were used in these calculations.

Meier, W. R., *Tritium Breeding Management in the HYLIFE Chamber* Lawrence Livermore National Laboratory, Livermore, Calif., UCRL-83969 (1980). See also *Nucl. Tech.* **52**, 170–178 (Feb. 1981).
Discusses design modifications that may be used to control the tritium-breeding ratio between 1.0 and 1.75.

Meier, W. R. and M. J. Monsler, *Parametric Studies of Inertial Confinement Fusion Economics*, Lawrence Livermore National Laboratory, Livermore, Calif., UCRL-82846, Summary (1979).
An analysis that couples LLNL's estimates of pellet performance with cost estimates for the major subsystems of a 1-GW_e inertial confinement fusion power plant to determine the cost of electricity.

Meier, W. R. and E. C. Morse, *A Nonlinear Simplex Method for Fusion Reactor Blanket Optimization*, Lawrence Livermore National Laboratory, Livermore, Calif., UCRL-90202, Summary (1984).
Discusses a method for optimization of blanket designs for fusion reactors.

Meier, W.R., *Multivariable Optimization of Fusion Reactor Blankets*, Lawrence Livermore National Laboratory, Livermore, Calif., UCRL-53543 (1984).
Describes blanket optimization method with applications to HYLIFE and Cascade.

Meier, W. R. and E. C. Morse, *Blanket Optimization Studies for the HYLIFE ICF Reactor*, Lawrence Livermore National Laboratory, Livermore, Calif., UCRL-91522 (1984).
Summary of HYLIFE example given in previous reference (UCRL-53543).

Meier, W. R. and W. B. Thomson, *Conceptual Design Considerations and Neutronics of Lithium Fall Laser Fusion Target Chambers*, Lawrence Livermore National Laboratory, Livermore, Calif., UCRL-80782 (1978). See also *Proc. 3rd ANS Top. Mtg. on Fusion* (Santa Fe, N. Mex., May 9–11, 1978).
Discusses important design considerations for the target chamber of a fusion power plant, emphasizing sizing, fail configuration, hydraulic effects, and neutronic and mechanical design considerations.

Meier, W. R. and J. A. Maniscalco, *Liquid Metal Requirements for Inertial Confinement Fusion*, Lawrence Livermore National Laboratory, Livermore, Calif., UCRL-80424 (1977). See also *Proc. Intern. Corrosion Forum* (Houston, Tex., March 6–10, 1978).
Surveys the potential applications of liquid metals on inertial confinement fusion. Lead, sodium, and lithium are compared.

Meier, W. R., N. J. Hoffman, and M. W. McDowell, *Liquid-Metal Aspects of HYLIFE*, Lawrence Livermore National Laboratory, Livermore, Calif., UCRL-84107 (1980). See also *Proc. 2nd Intern. Conf. on Liquid Metal Technol. in Energy Prod.* (Richland, Wash., April 20–24, 1980).
Discusses the liquid-lithium blanket and system that protects the structure of the HYLIFE reactor fusion chamber from the effects of the DT fusion reaction.

Meier, W. R. and J. A. Maniscalco, *Reactor Concepts for Laser Fusion*, Lawrence Livermore National Laboratory, Livermore, Calif., UCRL-79654 (1977). See also *Proc. Am. Instit. Chem. Engineers* (New York, N.Y., Nov. 13–17, 1977).
Discusses research on a liquid-lithium-cooled stainless steel manifold and a gas-cooled graphite manifold, and presents the liquid-lithium waterfall concept.

Monsler, M. J., *Final Optics for Laser Fusion Reactors*, Lawrence Livermore National Laboratory, Livermore, Calif., UCRL-80079, Abstract (1977).
Discusses the protection of the final focusing optics. Protection options and damage mechanisms are discussed for x rays, neutrons, and debris. A recommendation is made for a final focusing system that is compatible with the liquid-lithium-waterfall-reactor concept.

Monsler, M. J., *A Heavy Ion Beam Fusion Reactor Using Liquid Lithium Protected Chambers*, Lawrence Livermore National Laboratory, Livermore, Calif., UCRL-83424, Abstract/Summary (1979).

Describes an inertial fusion reactor concept that has the advantages of both liquid-metal reaction chambers and heavy-ion-beam drivers.

Monsler, M. J., *Progress in Inertial Fusion Reactor Design*, Lawrence Livermore National Laboratory, Livermore, Calif., UCRL-88733, Summary (1983).

Discusses recent reactor designs, pointing out advantages as well as potential engineering problems.

Monsler, M. J., *Reactor Studies for Inertial Fusion*, Lawrence Livermore National Laboratory, Livermore, Calif., UCRL-88299, Abstract (1982).

Describes the design techniques used to assure long vacuum-vessel life, considering both radiation damage and transient wall constraints.

Monsler, M. J., *Laser System Conceptual Design Issues for Commercial Laser Fusion Power Plants*, Lawrence Livermore National Laboratory, Livermore, Calif., UCRL-80180, Abstract/Summary (1977).

Discusses laser system design considerations with emphasis on power conditioning, beam quality, parasitic control, energy storage, and optical architecture combine to determine efficiency, scalability, and technical risk.

Monsler, M. J., *A Flourescence-Pumped Photolytic Gas Laser System For Commercial Laser Fusion Power Plant*, Lawrence Livermore National Laboratory, Livermore, Calif., UCRL-79655 (1977). See also *Proc. Am. Instit. Chem. Engineers Conf.* (New York, N.Y., Nov. 13–17, 1977).

Discusses the first results for the conceptual design of a short-wavelength gas laser system suitable to drive a commercial laser-fusion power plant. Includes a comparison of projected overall system efficiencies of photolytically excited oxygen, sulfur, selenium, and iodine lasers.

Monsler, M. J., *Laser Fusion: An Assessment of Pellet Injection, Tracking, and Beam Pointing*, Lawrence Livermore National Laboratory, Livermore, Calif., UCRL-80563 (1978). See also *Proc. 3rd Top. ANS Mtg. on Fusion* (Santa Fe, N. Mex., May 9–11, 1978).

Presents a conceptual design for a target injection and final optical system that can be integrated with a lithium waterfall laser fusion reactor, and can operate repetitively within specific tolerances.

Monsler, M. J. et al., *Electric Power From Laser Fusion: The HYLIFE Concept*, Lawrence Livermore National Laboratory, Livermore, Calif., UCRL-81259 (1978). *Proc. IECEC Conf.* (San Diego, Calif., Aug. 20-25, 1978).

Describes an ICF chamber design that calls for the use of common ferritic steels, low-risk metal technology, and a power density approaching that of a fission reactor.

Monsler, M. J. and J. A. Maniscalco, *Optical Design Considerations for Laser Fusion Reactors*, Lawrence Livermore National Laboratory, Livermore, Calif., UCRL-79990 (1977). See also *Proc. 21st Annual Technol. Symp. Soc. of Photo-Optical Instrumentation Engineers (SPIE)* (San Diego, Calif., Aug. 22–26, 1977).

Discusses the plan for the development of commercial inertial confinement fusion power plants, emphasizing the conceptual design for a liquid-lithium fall reactor, damage mechanisims, and protection techniques.

Monsler, M. J. and W. R. Meier, *Inertial Fusion Reactor Studies at LLNL*, Lawrence Livermore National Laboratory, Livermore, Calif., UCRL-87532 (1982). See also *Proc. 12th Symp. Fusion Technol.* (Jülich, FRG, Sept. 13–17, 1982).

Presents the results of reactor studies for ICF energy production. Variants of the same basic design—HYLIFE—can be used for electricity production, fissile fuel production, or tritium breeding.

Monsler, M. J. and W. R. Meier, *A Conceptual Design Strategy for Liquid-Metal-Wall Inertial Fusion Reactors*, Lawrence Livermore National Laboratory, Livermore, Calif., UCRL-84881 (1980). See also *Nucl. Eng. Des.* **63**, 289–313 (1981).

A review of the development and design of liquid-metal-wall chambers over the past decade, using the perspective of formulating a conceptual design strategy for such chambers.

Monsler, M. J. et al., *Electrical Power From Inertial Confinement Fusion: The HYLIFE Concept*, Lawrence Livermore National Laboratory, Livermore, Calif., UCRL-81866 (1978). See also *Proc. Heavy Ion Inertial Fusion Workshop* (Argonne National Laboratory, Argonne, Ill., Sept. 19–26, 1978).

Describes a HYLIFE energy chamber that can be conceptually operated using less than one percent of the gross thermal power to circulate the lithium. A lithium blanket protects the structure. Design concept calls for use of common ferritic steels and a power density approaching that of a LWR.

Monsler, M. J. et al., *Electric Power From Laser Fusion: The HYLIFE Concept*, Lawrence Livermore National Laboratory, Livermore, Calif., UCRL-81259 (1978).

This report describes a high yield lithium injection fusion energy chamber that can be operated conceptually with pulsed yields of several thousand megajoules a few times per second, using less than 1% of the gross thermal power to circulate the lithium.

Pitts, J. H., *Fatigue-Crack Growth in Inertial Confinement Fusion Reaction Chamber Components*, Lawrence Livermore National Laboratory, Livermore, Calif., UCRL-87185 (1982). See also *Nucl. Technol./Fusion*, **4**, 967–972 (1982).

Outlines a three-step method for analyzing fatigue-crack growth under of both steady and fluctuating load conditions. Analysis of the HYLIFE reaction chamber shows that it is feasible to manufacture components free from the defects that could potentially limit chamber lifetime.

Pitts, J. H., *Heat-Transfer Limitations on Pellets Used in ICF Reaction Chambers*, Lawrence Livermore National Laboratory, Livermore, Calif., UCRL-85975 (1981). See also *Proc. 9th Symp. on Eng. Problems of Fusion Research* (Chicago, Ill., Oct. 26–29, 1981).

A spherically symmetric, transient heat-transfer analysis conducted on cryogenic multiple-shelled laser-driven pellets shows that injection velocities of 300 m/s are required.

Pitts, J. H., *A Consistent HYLIFE Wall Design That Withstands Transient Loading Conditions*, Lawrence Livermore National Laboratory, Livermore, Calif., UCRL-84271 (1980). See also *Proc. 4th ANS Top. Mtg. on the Technol of Controlled Nucl. Fusion* (King of Prussia, Penn., Oct. 14–17, 1980).

A discussion of the First Structural Wall (FSW) design. A 50-mm-thick FSW located at a 5-m radius is capable of lasting the chamber's entire 30-year lifetime.

Pitts, J. H., *Fatigue Crack Growth in HYLIFE Reaction Chamber Components*, Lawrence Livermore National Laboratory, Livermore, Calif., UCRL-86364, Summary (1982). See also *Fatigue-Crack Growth In Inertial Confinement Fusion Reaction Chamber Components*, Lawrence Livermore National Laboratory, Livermore, Calif., UCRL-87185 (1982).

Discusses fatigue-crack growth in critical areas of the HYLIFE reaction chamber.

Pitts, J. H. et al., *Engineering Design Characteristics of the HYLIFE Reaction Chamber For Laser Fusion*, Lawrence Livermore National Laboratory, Livermore, Calif., UCRL-83425, Summary (1979).

Explains HYLIFE reaction chamber design characteristics.

Pitts, J. H., J. Hovingh, and S. Walters, *Inertial Confinement Fusion*, Lawrence Livermore National Laboratory, Livermore, Calif., UCRL-87644 (1982). Reprinted from *Mech. Eng.* **104**(10) (Oct. 1982).

Discusses inertial confinement approach to fusion energy, including LLNL's state of the art fusion experiments and the results achieved through the use of neodymium-doped glass lasers.

Pitts, J. H. et al., *Potential Design Modifications for the HYLIFE Reaction Chamber*, Lawrence Livermore National Laboratory, Livermore, Calif., UCRL-82895 (1979). See also *Proc. 8th Symp on Eng. Problems of Fusion Research* (San Francisco, Calif., Nov. 13–16, 1979).

Discusses design modifications for the HYLIFE reactor, liquid-lithium circulation, and the advantage of jets over solid annulus or concentric annuli.

Pitts, J. H. and I. V. Ojalvo, *Fluid and Structural Dynamic Design Considerations of the HYLIFE Nozzle Plate*, Lawrence Livermore National Laboratory, Livermore, Calif., UCRL-84874 (1981). See also *Proc. 6th Intern. Conf. on Structural Mech. in Reactor Technol. (SMIRT)* (Paris, France, Aug. 17–21, 1981).

The key element in the reaction chamber that produces the jet array is the nozzle plate. This paper presents a description of the design and analysis of a nozzle plate that can withstand the structural loads and permit the fluid jet array to be reestablished for a 1-Hz fusion reaction frequency.

Pitts, J. H. and I. V. Ojalvo, *Design Considerations of the HYLIFE Nozzle Plate*, Lawrence Livermore National Laboratory, Livermore, Calif., UCRL-87066 (1981). See also *Res Mechanica Letters* 5, 231–236 (1982).

The HYLIFE reaction chamber uses a 0.5-m-thick, 10-m-diam nozzle plate to create a liquid metal jet array. This paper discusses fluid and structural dynamic considerations, stress-scaling laws, and results.

Rockwell International Corporation, *Conceptual Design Study of the HYLIFE Lithium Fall Laser Fusion Chamber*, Lawrence Livermore National Laboratory, Livermore, Calif., UCRL-15219 (1979).

Detailed weight analysis, assembly sequence, chamber vibration analysis, splash baffle stress study, and an analysis of the first wall thermal stresses. Also, new concepts pertaining to the first wall, the lithium inlet nozzle, the chamber supports, the inlet piping, and pressure vessel.

Ross, M. et al., *An Application of Fluid Metal Theory to Inertial Confinement Fusion Reactor Studies*, Lawrence Livermore National Laboratory, Livermore, Calif., UCRL-87713 (1982).

Analyzes the equations of state and transport properties for fluid metal in inertial confinement fusion reactors.

Sherohman, J. W. and W. R. Meier, *A Parametric Study of a Target Factory for Laser Fusion*, Lawrence Livermore National Laboratory, Livermore, Calif., UCRL-84264 (1980). See also *Proc. Am. Nucl. Soc. Top. Mtg. on the Technol. of Controlled Nucl. Fusion* (King of Prussia, Penn., Oct. 14–17, 1980).

Analyzes a target factory. Rate equations are developed to identify key parameters, attractive production techniques, and cost-scaling relationships for a commercial target factory.

Sherohman, J. W., *Parametric Expressions of Tritium Flow Rates and Inventories on a Target Factory*, Lawrence Livermore National Laboratory, Livermore, Calif., UCID-18877 (1980).

Parametric expressions are derived for tritium flow rates and inventories in a target factory, and a parametric study to determine the amount of tritium involved in the target factory of an ICF power plant.

Walker, P. E., *Remote Systems Requirements of the High Yield Lithium Injection Fusion Energy (HYLIFE) Converter Concept*, Lawrence Livermore National Laboratory, Livermore, Calif., UCRL-81309 (1978). See also *Proc. Am. Nucl. Soc. 1978 Winter Mtg.* (Washington, D.C., Nov. 12-16, 1978)

Describes ideas for remote maintenance of laser beam blast baffles, optics, and target material traps.

U. S. Government Printing Office: 1986/2-687-002/44041